HYPERBOLIC REPRESENTATION OF FORCE VERSUS DISPLACEMENT RELATIONSHIP FOR LATERAL PIPE MOVEMENT IN DRY SOIL

by

Richard D. Yovichin III

Submitted in Partial Fulfillment of the Requirements

for the Degree of

Masters of Science in Engineering

in the

Civil and Environmental Engineering

Program

YOUNGSTOWN STATE UNIVERSITY

August, 2018

Hyperbolic Representation of Force versus Displacement Relationship for Lateral Pipe Movement in Dry Soil

Richard D. Yovichin III

I hereby release this thesis to the public. I understand that this thesis will be made available from the OhioLINK ETD Center and the Maag Library Circulation Desk for public access. I also authorize the University or other individuals to make copies of this thesis as needed for scholarly research.

Signature:

_____

Richard D. Yovichin III, Student Date

Approvals:

_____

Dr. Jai K. Jung, Thesis Advisor Date

_____

Dr. AKM Islam, P.E., Committee Member Date

_____

Dr. Richard Deschenes, Committee Member Date

_____

Dr. Salvatore A. Sanders, Dean of Graduate Studies Date

ABSTRACT

Research and engineering practices for an earthquake response of underground pipelines has focused on permanent and transient ground deformation (PGD and TGD) effects, with the recognition that PGD often causes the most serious local damage in buried pipeline networks. The effects of permanent ground deformation not only apply to earthquakes, but also occur in response to floods, landslides, tunneling, deep excavations, and subsidence caused by dewatering or the withdrawal of minerals and fluids during mining and oil production. Such loading conditions are becoming more important as the needs for technology development increase to combat issues regarding natural hazards, human threats, and construction in congested urban environments.

Of key importance in this research is the soil and pipeline interaction with respect to PGD below subsurface. This response is typically highlighted by force vs. displacement relationship and is primarily a function of soil density, depth, and diameter of pipe. The force vs. displacement relationships for transverse horizontal force on pipelines subjected to lateral ground movement are represented by a hyperbola. Transforming such hyperbola into a linear representation can make analysis of soil-pipe interaction much easier. This process allows for the development of a simplistic model representing a wide range of soil characteristics.

The development of this simplified, yet practical, nonlinear force vs. displacement relationship for lateral pipe movement, using hyperbolic parameters, is useful to engineers. This approach is convenient for modeling the soil-pipe interaction and is critical for addressing the complexities of soil and pipe performance, consistent with real-world soil-pipe behavior, by illustrating the minimum soil control design and the maximum soil resistance.

ACKNOWLEDGEMENTS

I would like to express a sincere appreciation for Youngstown State Factuality that provided insight threw this whole experience, directly or indirectly. First and foremost, I would like to express my deepest gratitude to my supervisor, Dr. Jai K. Jung. He has provided me with instrumental guidance and encouragement throughout this graduate program. This research experience would not have been possible without his continuous support and guidance.

I would also like to thank Dr. Richard Deschenes and Dr. AKM Anwarul Islam, P.E. for serving as thesis committee members, in regards to their recommendations and advice during this research work. Furthermore, this research experience was possible due to funding through the Cushwa Fellowship.

Finally, I would like to takes this opportunity to express my greatest gratitude for my loving family, who has offered encouragement and words of wisdom throughout this endeavor. Additionally, I need to mention my sincerest appreciation for the entire faculty at Youngstown State and my colleagues, who provided me with guidance at various stages of this research.

TABLE OF CONTENTS

LIST OF FIGURES

LIST OF TABLES

Chapter 1. Introduction

1.1. General Overview

Earthquake-, flood-, and landslide-induced permanent ground deformation (PGD) often involves large, irrecoverable soil distortion with geometric soil mass changes and large plastic pipeline deformation, involving both material and geometric nonlinearities (O'Rourke et al., 2004; Jung et al., 2013a; Jung et al., 2016). Such behavior imposes significant demands on modeling of soil-pipe interaction. The soil-pipe interaction under PGD is often performed with one-dimensional finite element models to represent the pipeline and soil force vs. displacement relationships that are mobilized by various types of ground movement. As described by several design guidelines and previous researchers (e.g., ASCE, 1984; Trautmann et al., 1985; American Lifelines Alliance, 2005), soil pipeline interaction is represented by components in the axial, transverse, and vertical bearing directions, as represented by the soil springs (Wijewickreme et al., 2009). This approach benefits from ease of application and its incorporation in available finite element codes (ASCE, 1984; ABAQUS, 2017), but suffers from the uncoupled representation of soil as a series of spring-slider reactions (Honegger and Nyman, 2004; Jung et al., 2013b).

Many researchers have developed soil-pipe force vs. displacement relationships, more realistically, using advanced numerical analysis (e.g., Wong and Duncan, 1974; Trautmann and O'Rourke, 1983; Yimsiri et al., 2004; Robert et al., 2016), but they require a significant computational power and an in-depth understanding of numerical

modeling. Thus, providing a simplified hyperbolic method, to represent soil-pipe behavior, may allow for a user-friendly and relatively quick process based on numerous experimental data as an alternative to advanced numerical analysis.

1.2. Background

The overall trend of a force-displacement curve for soil-pipe interaction changes as a function of soil types and confining stress around the pipe. Typically, loose to medium sand, force-displacement curve, rises nonlinearly as the curve converges to a maximum force with substantial displacements at the asymptote. The initial nonlinear portion of dense to very dense force-displacement graph rise to a peak value, F_{max}, then shows a softening behavior, and enters to a critical stage where force remain constant as the displacement increases. Trautmann and O'Rourke (1983) discussed these trends of soil-pipe behavior.

Researchers have been working to represent such high nonlinear behavior of soil-pipe interaction in a mathematical model such as the Nor-sand, Mohr-Coulomb, Cam-Clay, or Drucker-Prager models. In this study, a hyperbolic model will be used to represent the soil-pipe interaction for lateral pipe movement in dry sand. Many researchers have described the nonlinear curve of soil-pipe interaction with a rectangular hyperbola involving problems associated with stress-strain behavior (Konder, 1963; Duncan and Chang, 1970; Wang and Duncan, 1974), loads on piles (Fellenius, 1980), responses involving vertical anchors (Das and Seeley, 1975), and pipes under the conditions of lateral loading (Audibert and Nyman, 1977; Trautmann and O'Rourke, 1983).

There are benefits of transforming an experimental force-displacement curve into a hyperbolic representation. This simplified representation is useful for both hand calculations, as well as, numerical analysis of soil pipe interaction (Trautmann and O'Rourke, 1983).Trautmann and O'Rourke (1983) defined the hyperbola in its general form as:

$$F = \frac{Y}{A+BY} \tag{1.1}$$

Where F is the force and Y is the displacement. The variables A and B describe the inverse slope of the curve at the origin and the inverse force value of the asymptote, respectively.

A typical hyperbolic model was applied and the results are summarized in Figure 1-1. A theoretical force-displacement relationships for loose to medium and dense to very dense sands are shown here. By plotting the data in dimensionless form (normalized form), it allows for predictive use that is helpful in creating a generalized hyperbolic model. This hyperbolic model can be created in terms of a ratio with any variability of the tests; such as pipe diameter, depth, length, and unit weights of the soils (Trautmann and O'Rourke, 1983). Therefore, as shown in Figure 1-1, the displacement was plotted as a double-normalized constant Y'/Y'_{max} , and F'/F'_{max} as the force. F'_{max} is the maximum dimensionless force and the corresponding maximum displacement is Y'_{max} associated with failure. Including the dimensionless displacement (Y'), as the top horizontal axis,

allows for displacement differences between soil types to be shown (Trautmann and O'Rourke, 1983). Similarly, dimensionless force can be referred to F'.

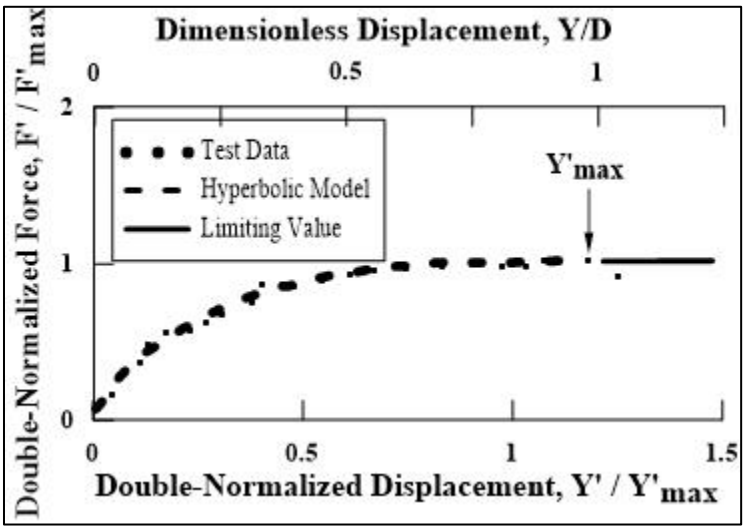

a) Loose to Medium Sand

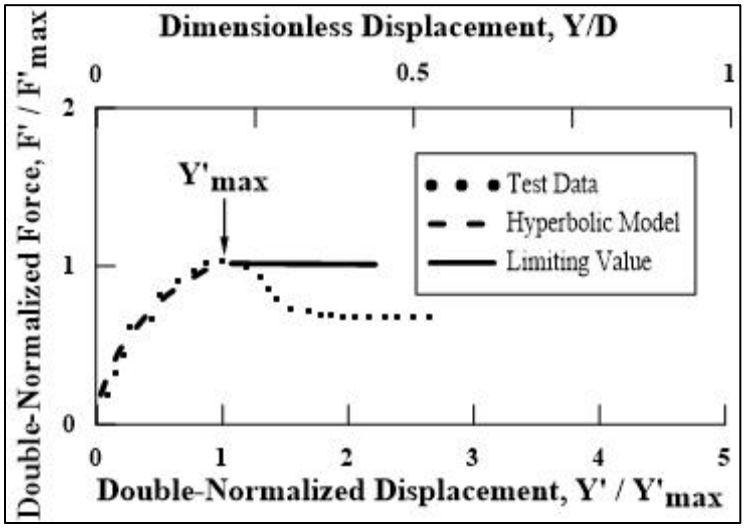

b) Dense to Very Dense Sand

Figure 1-1: The force with respect to displacement relationship for application of a hyperbolic model illustrating various soil types (After Trautmann and O'Rourke, 1983).

As discussed earlier, the force-displacement curve has a gradual increase, for loose to medium sand; the actual curve can be closely approximated by the hyperbolic curve. This hyperbola passes through the point (Y'_{max}, F'_{max}). For dense to very dense sands, as shown in Figure 1-1b, the hyperbola characterizes the actual curve for displacement less than Y'_{max}. A limiting force of F'_{max} is used for displacement greater than Y'_{max}, For dense to very dense sands, the use of the limiting value in the hyperbolic model at large displacement overestimates the actual force exerted on the pipe. Therefore, the hyperbolic model gives a conservative estimate for problems associated with large ground deformation (Trautmann and O'Rourke, 1983).

1.3. Research Objective

The overall goal of this study is to represent the soil-pipe behavior using hyperbolic parameters. The hyperbolic parameters will change as a function of other soil parameters such as unit weight. This will be done by transforming experimental data, from various researchers, into a dimensionless form and using a normalization process plotted on a transformed axis. The transformed axis plot allows for two parameter to be generated from each soil type, ranging from loose to very dense sands. The parameters (A and B) are generalized in Equation 1.1.

Chapter 2. Literature Review

2.1. Previous Experimental Research

Hansen (1953) conducted experiments to understand how soils-structures interacted when modeling retaining walls under passive lateral movement with loose backfill sand. The main objective of his research was to identify patterns and mechanisms associated with failure. The experimentation model Hansen (1953) used was a small-scale box with clear windows. To measure wall displacement, a camera was positioned outside of the window to take photographs. A limitation of his research was, he did not take into account passive soil forces on the wall. Hansen (1961) continued this research and focused his attention on passive soil forces on lateral loaded piles in sand.

Ovesen (1964) performed a series of tests in loose and dense sands to simulate plain strain conditions. He chose different overburden ratios, from 1 to 10, to encompass deep and shallow failure mechanisms. An analytical model was created from the test results to estimate passive soil loads on anchors. Ovesen and Stromann (1972) reported and summarized the information obtained from Ovesen (1964), as well as, the analytical model.

The behavior of vertical deadman anchors on port structures, in loose and dense sands under saturated an unsaturated conditions, were investigated by Kosteyukov (1967). The researcher focus was on how soil density in front of the anchor varied from soil type. After testing, his findings indicated that soil density in front of the plate, for dense sand, remained nearly constant during pullout. The loose test, however, exhibited a different

trend. The soil density in front of the anchor increased in a triangular fashion in front of the anchor during movement.

Neely et al. (1973) conducted laboratory tests on vertical anchors in loose sand with a friction angle of 35°. Their results were then compared with the findings from Smith (1962) on deadman anchors in loose sand, along with other theoretical approaches. An analytical model using Sokolovskii (1965) method of stress characterization was found to be in agreement with the findings from Neely et al. (1973). They also found that plates under plain strain conditions, when the plates width to height ratio (aspect ratio) of five, failed in the ranges of 0.1D and more than 0.2D of displacement, where D is the depth of the anchor. This finding can be applied to overburden ratios (depth of the bottom of the plate to the height of the plate) of one to five, respectively.

Das and Seeley (1975) investigated how aspect ratios affected horizontal movement on vertical anchors. A single rectangular hyperbola (Equation 2.1) was found to approximate the dimensionless force-displacement curve caused by the horizontal movement. Various researchers have used the rectangular hyperbola in the development of analytical modeling using "soil springs". Their findings indicated, that as the aspect ratio increased the load per unit width of the anchor decreased.

$$\overline{P} = \frac{\overline{Y}}{0.145+0.855\,\overline{Y}} \tag{2.1}$$

Where:

$\overline{P}$ = lateral anchor load due to soil divided by the lateral anchor load due to soil at failure

$\overline{Y}$ = displacement of anchor horizontally divided by displacement of anchor horizontally at failure

Buried steel pipes in soils, under lateral loads, were physically tested by Audibert and Nyman (1975, 1977). The pipe diameters used in their tests were as follows 25 mm, 60 mm, and 114 mm. The overburden ratios, they investigated, were in a wide range from 1.5 to 24.5. To validate their physical laboratory tests, they conducted a field test. By using Hansen's (1961) analytical findings and recommendations, Audibert and Nyman (1977) concluded that their results were in agreement with Hansen (1961), as well as, Das and Seely (1975). Audibert and Nyman (1977) formulated a rectangular hyperbola (Equaton 2.2) from the dimensionless force-displacement curve to represent lateral loads on pipes, which was independent from the hyperbola reported from Das and Seely (1975).

$$\frac{Y''}{F''} = 0.145 + 0.855Y'' \qquad (2.2)$$

Where:

Y" = Dimensionless displacement / Dimensionless displacement at failure

F" = Dimensionless force / Dimensionless force at failure

As the sand density and pipe size decreased, the normalized displacement occurring at failure increased, another finding reported by Audibert and Nyman (1977).

2.2. Experimental Research Used in This Study

Trautmann and O'Rourke (1983, 1985) conducted tests on lateral loaded pipes with overburden ratios ranging from 2 to 11. The series of tests also involved three unit weights of soils with pipe diameters of 102 mm and 324 mm. The scope of their research was to investigate how depth and unit weight of soils effect a force-displacement curve for a laterally loaded pipe. The results from their experimentation, for medium and dense sand, were compared with an analytical model developed by Rowe and Davis (1982) and more recently, by Jung et al. (2013b) with very good agreement. For loose sand, however, the loads were found to be more than the loads estimated by the analytical model and similar to the loads produced by the analytical model for medium sand. Trautmann and O'Rourke (1983) derived three hyperbolic curves describing the average for each of the three soil densities tested (14.8 kN/m^3, 16.4 kN/m^3, and 17.7 kN/m^3) and are as follows:

$$\frac{Y''}{F''} = 0.15 + 0.85Y'' \tag{2.3}$$

$$\frac{Y''}{F''} = 0.1 + 0.9Y'' \tag{2.4}$$

$$\frac{Y''}{F''} = 0.25 + 0.75Y'' \tag{2.5}$$

Hsu (1993) performed a series of test on two soil types with overburden ratios ranging from 1.5 to 20.5. These tests used two pipe diameters, 38.1 mm and 76.2 mm. Hsu's (1993) findings for the maximum soils loads were between the results founded by Trautmann and O'Rourke (1983) and those of Audibert and Nymann (1977). Hsu (1993) investigated the relationship between strain-rate and maximum soil loads on pipe. This allowed Hsu (1993) to develop a power law relationship between the two. By using different strain rates found from the soil loads and pullout rates, he developed a series of rectangular hyperbolic relationships.

Turner (2004) performed experiments using sieved glacio-fluvial, well graded sand (referred to as RMS graded sand) for dry and partially saturated conditions. The density of the dry soils ranged from 16.9 kN/m^3 to 17.2 kN/m^3. The compaction of the soil was checked by using a nuclear gage, which allows for greater accuracy. He provided possible correction to the curves presented by Trautmann and O'Rourke (1983). The results from his testing were slightly higher than Trautmann and O'Rourke (1983). Therefore, he provided modifications to the charts presented by Trautmann and O'Rourke (1983) for soil loads of pipes below subsurface in dry sand. In addition, Turner (2004) provided force-displacement curves for soils with 4 ~ 10% moisture content and concluded that moist soil loads can be as high as double when compared to dry sand.

Karimian (2006) modified a test chamber to accommodate larger diameter steel pipes. He developed instrumentation capable of recording normal stresses, pullout resistance,

displacements of geosynthetics, pipes, and sand grains during testing, and deformation occurring at the surface. A clamp was attached at the end of each pipe and a shackle was connected to clamp. A cable attached the shackle to the load cell and the load cell was used to measure the force. The displacement of the pipe was measured using a string potentiometers attached to the cables located outside of the box (Karimian, 2006). He performed axial and lateral pullout tests on trenched backfill and geotextile-lined trenches; while developing a model for comparison. He found that geosynthetic-wrapped pipes decreased axial soil loads. He also mentioned that the lateral loading tests were consistent with the rectangular hyperbola reported by Das and Seeley (1975) and described by Trautmann and O'Rourke (1983). Karimian (2006) suggested the findings described by Trautmann and O'Rourke (1983) and Turner (2004) were slightly high when predicting soil loads on pipes. Karimian (2006) reported that geotextiles in trenches allows for soil loads in a lateral direction to decrease. The model was developed using a modified hyperbolic function for transverse ground movement. The trenched geotextiles analytical model soil loads were slightly higher than the tests performed, and Karimian (2006) stated that this occurrence could be due to localized shear failure.

The purpose of Olson's (2009) research was to understand the factors influencing soil performance in soil-pipe interaction, and to improve accuracy of large-scale testing. A nuclear gage and density scope were used to measure a unit weight of dry and partially saturated RMS graded sand. The comparison of the unit weight using two different methods agrees very well and Olson (2009) suggested using the nuclear gage for large-scale tests because it is easy to use and a relatively quick process. Also, to measure

normal stress during experimentation, tactile pressure sensors are dependable and accurate.

Daiyan et al. (2011) investigated axial-lateral interaction of pipes, on a series of four tests with different angles of movement, using a centrifuge model. The angles of movement were 90°, 0°, 40°, and 70°. The ends of the pipe were connected to a load cell. This load cell was then connected to a leadscrew actuator that allowed for horizontal plain-strain movement of the buried pipe. A displacement laser measured the displacement of the buried pipe, as the load was applied (Daiyan et al., 2011). Daiyan et al. (2011) further compared the centrifuge tests with the results from the numerical model. The finding suggested that oblique angles, less than 40°, equated to an axial load increase up to 2.5 times. The ultimate loading results from the axial-lateral centrifuge testing were in agreement with the numerical model, conversely, the ultimate displacement between the numerical and the experimental were not consistent. Daiyan et al. (2011) suggested the ultimate displacement discrepancy was due to the test-bed preparation of the centrifuge; while the numerical findings were consistent with the common industrial procedures and cited works. They proposed that an updated pipe-soil model is needed to address complexities associated with soil restraints and the variability of pipe movement.

Almahakeri et al. (2013) performed six lateral loaded tests on two types of GFRP (E-glass fiber and epoxy resin). The over-burden ratios were 3, 5, and 7. The pipe diameters for GFRP were 115 and 114 mm. The strength, deflection, and failure modes of GFRP pipes were compared with steel pipe tests conducted by Almahakeri et al. (2012). The

diameter of the steel pipes were 105 mm. Almahakeri et al. (2013) concluded that the peak loads of GFRP pipes were similar to steel with similar H/D ratios. These peak loads increased as a function of depth. Due to the flexibility of GFRP pipes, there longitudinal bending is 4 to 7.5 times greater than steel pipes.

A series of lateral loaded pipes in olivine sands were tested by Burnett (2015). Burnett (2015) developed a large-scale testing facility to focus on horizontal soil-pipe interaction. His testing apparatus was capable of reducing sidewall friction. To measure the displacement, the testing apparatus was designed with a viewing window. The window was retrofitted with a camera and software processed imaging was used (Burnett, 2015). In addition, a digital image correlation was able to collect high quality data; describing complex strain-soil behavior. As previously mentioned by others research, he observed that an increase in lateral forces is a function of depth and diameter of pipe. When comparing pipe diameters, he noted that comparing uplift to diameter percentages increased as a function of size. Lastly, he suggested that loose sand requires large pipe displacement to initiate the soil failure mechanism. This displacement causes the soil in front of the pipe to densify, creating a wedge shape comparable to the results found in dense sand.

Robert et al. (2016) performed two separate test, under both dry and unsaturated conditions with two types of soils. Fine Chiba sand (Robert 2010; Robert and Soga 2013; Fern et al. 2014a, b) and coarser RMS graded sands (Jung et al. 2013b; O'Rourke 2010) were used in these tests. The results from the tests were compared with the numerical or

finite-element (FE) simulation results. The peak load for unsaturated Chiba sand experiments were greater than the load for dry sand. The RMS graded sand had nearly the same peak load for unsaturated as for the dry sand conditions, however, the peak load for the unsaturated condition was 10 % higher. The unsaturated soil model results were similar for both cases where the pre-failure stiffness of the unsaturated condition was greater than the dry condition, which agrees with Jung et al (2013b). The types of soils used were found to effect the mechanical behavior and was more apparent in the finer Chiba sand by having a higher maximum peak force.

Chapter 3. Methods

3.1. Data Collection

The soil-pipe interaction test data for this research was collected from various researchers including Trautmann & O'Rourke (1983), Hsu (1993), Turner (2004), Karimian (2006), Olson (2009), Daiyan et al. (2011), Almahakeri et al. (2013), Burnett (2015), and Robert et al. (2016). In addition to the existing test data, eight additional new tests performed by Li (2016) were used. The data from Trautmann and O'Rourke (1983), Turner (2004), Olson (2009), and Li (2016) was obtained from the actual researcher. While the data from Hsu (1993), Karimian (2006), Daiyan et al. (2011), Almahakeri et al. (2013), Burnett (2015), and Robert et al. (2016) was digitized from their published works.

The experiments were performed in a wide range of dry soil type with various pipe diameter under plane-strain, lateral loading conditions. To facilitate the comparison of

experimental results under different condition, the measurements output were converted to dimensionless form. The dimensionless format also facilitates the application of the results to a variety of pipe diameter and depth conditions of practical interest. Figure 3-1 is a typical generalized dimensionless force-displacement curve for lateral pipe movement. Shown on the vertical axis is the lateral force imposed on the pipe by relative lateral displacement in sand, which is expressed as $F' = F / (\gamma_d H_c DL)$, in which F is the measured lateral pipe force, γ_d is the dry unit weight of the sand, H_c is the depth from the top of the soil to the center of the pipe, D is the external diameter of kthe pipe, and L is the length of the pipe involved in the test. The horizontal axis is the dimensionless pipe displacement expressed as $Y' = Y/D$, in which Y is the measured relative lateral pipe movement.

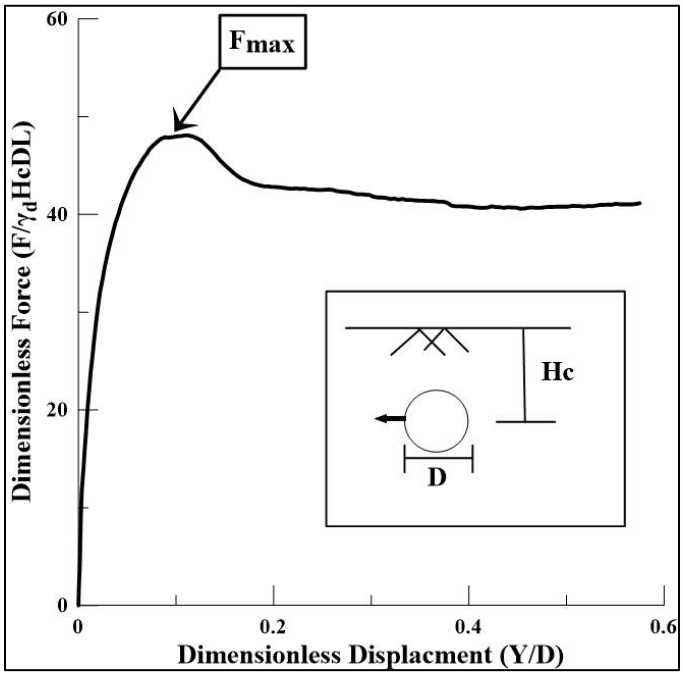

Figure 3-1: Generalized Dimensionless Force-Displacement Curve for Lateral Pipe Movement.

This study categorized soils into four classifications; loose, medium, dense, and very dense soils. Each soil classification were categorized by γ_d; <16 kN/ m^3, 16-16.7 kN/m^3, 16.7-17.5 kN/m^3, and >17.5 kN/m^3, respectively. More details about each soil type are described under the subheadings, as follow:

3.1.1. Loose Sand

As mentioned previously, loose soils were defined as having a γ_d < 16 kN/m^3. Data analysis was performed on twenty-eight tests. Of these test, nine were from Hsu (1993), six from Almahakeri et al. (2013), four from Burnett (2015), and one from Daiyan et al. (2011) and Robert et al. (2016).

Hsu (1993) performed tests with varying Hc/D, from 2 to 20, for loose dry sands. Hsu (1993) used a test box with the dimensions of 1.8 m x 1.8 m x 1.2 m. The diameters of pipes ranged from 38.1 mm to 228.6 mm. Pipe movement velocities ranged from 1.4 mm/min to 726 mm/min, which were controlled by a gearbox. A linear variable differential transducer (LVDT) measured the force and displacements. A data acquisition system recorded the values obtained from the LVDT. The soils were spread by using a spreading hopper (Hsu, 1993).

Almahakeri et al. (2013) performed six tests. These tests were performed on GFRP (E-glass fiber and epoxy resin pipe) in a test pit 4 m x 2 m x 2 m. This experiment was

accomplished by the use of two parallel cable, tied at each end. These cables were then attached to a hydraulic actuator. The actuator caused the pipe to move in a longitudinal direction.

Burnett (2015) performed thirteen tests on loose sand, however, only four tests exceeded and Hc/D greater than 1. Burnett (2015) testing apparatus was designed using a similar approach described by Trautmann and O'Rourke (1983) and Audibert and Nyman (1975). The test pit dimensions were 6.4 m x 2.7 m x 1.8 m. A hydraulic actuator applied the load to the pipe, while a load actuator measured the load. To measure the displacement, the testing apparatus was designed with a viewing window. The window was retro-fitted with a camera and software processed imaging was used (Burnett, 2015).

Robert et al. (2016) investigated lateral displacement using the split-box method. Robert et al. (2016) describes how the experiment process was followed but fails to mention the pipe length (L). An assumption describing the pipe length of 2.03 m was made, and summarized in Table 3-1. This assumption was based upon the spit-box dimensions being 3.0 x 2.03 x 2.02 m. The pipe was located parallel to the wall measuring 2.03 m, which would be the minimal length necessary for this type of experiment. Please note that the above assumption is summarization purpose for Table 3-1 only. Robert et al. (2016) reported the force as force per unit length (kN/m); therefore, L was taken as 1 m when transforming his test data into a dimensionless force vs. dimensionless displacement graph as seen in Figure 3-2.

Daiyan et al. (2011) investigated axial-lateral interaction of pipes using a centrifuge model. Since the lateral movement of pipe is the primary scope of this research, an angle equal to 90^{o} was used. This specification equated to the use of only one test ($\theta = 90°$). The centrifuge chamber pit was 1.18 m x 0.940 m x 0.400 m. A load cell was connected at each end of the pipe. This load cell was then connected to a leadscrew actuator that allowed for horizontal plain strain movement of the buried pipe. A displacement laser measured the displacement of the buried pipe as the load was applied (Daiyan et al., 2011).

Figure 3-2 highlights the overall trend of dimensionless force vs. displacement curve for twenty-two loose soil tests obtained from five independent research groups. Of these twenty-two tests, the Hc/D ratio greater than 1 was used in this research. At lower Hc/D, the diameter of pipe affects the normalized force as discussed in Jung et al. (2013a and 2013b). Such behavior is not under the scope of this research. To generate Figure 3-2, every parameter defined above was of concern. Back calculation was of primary concern in regards to Hsu (1993) data, because Hsu (1993) normalized force using the burial depth H, which is the distance from the surface to the bottom of pipe. Please note that Hc, defined from the surface to the centerline of pipe, was used in this study. The back calculations were accompanied by forward calculation to create a dimensionless graph as shown in the figure.

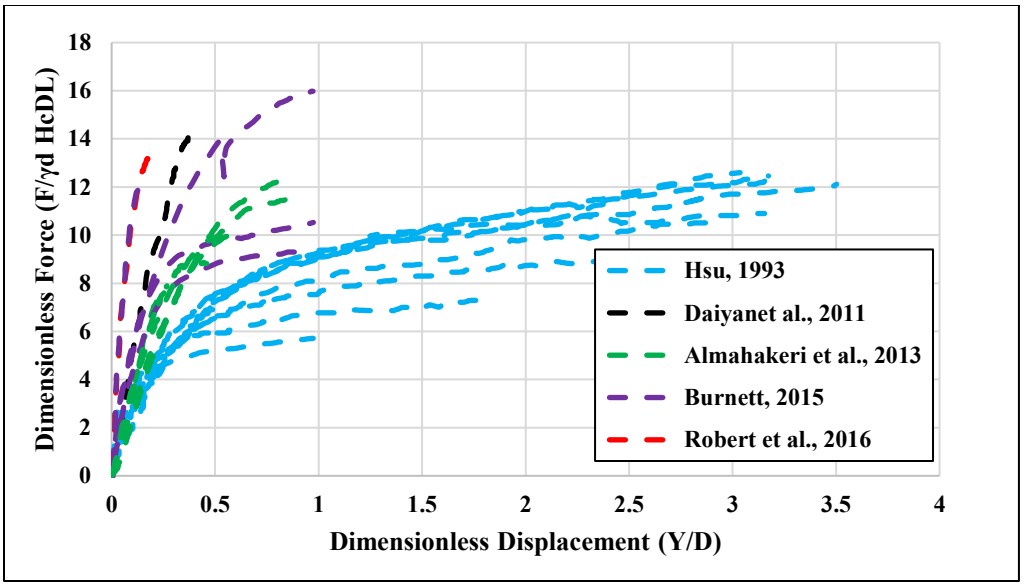

Figure 3-2: Loose sand data collected from various researches with a γ_d ranging from 14.6 kN/m^3 to 15.68 kN/m^3.

Table 3.1 summarized the parameters accounted for in each test, specified by each researcher. The information inputted in the table is placed in sequential order from least to greatest for varying γ_d, under the umbrella of loose sand. As described above, γ_d is defined as < 16 kN/m^3 for loose sand. As seen in the table, the range for Hc/D is 2 to 20.

Table 3-1: Individual parameter, for each experiment, from various researcher on loose sand.

γ_d (kN/m^3)	Length (mm)	Diameter (mm)	Hc/D	Experiment
15	1824	114	3	Almahakeri et al. (2013)
15	1840	115	3	Almahakeri et al. (2013)
15	1824	114	5	Almahakeri et al. (2013)
15	1840	115	5	Almahakeri et al. (2013)
15	1824	114	7	Almahakeri et al. (2013)
15	1840	115	7	Almahakeri et al. (2013)
14.6	914	254	3	Burnett (2015)
14.7	914	254	3	Burnett (2015)
14.8	914	254	7	Burnett (2015)
15.4	914	254	3	Burnett (2015)
15.2	1200	38.1	2	Hsu (1993)
15.2	1200	38.1	4	Hsu (1993)
15.2	1200	38.1	6	Hsu (1993)
15.2	1200	38.1	8	Hsu (1993)
15.2	1200	38.1	10	Hsu (1993)
15.2	1200	38.1	12	Hsu (1993)
15.2	1200	38.1	14	Hsu (1993)
15.2	1200	38.1	16	Hsu (1993)
15.2	1200	38.1	20	Hsu (1993)
15.3	2030	114.6	5.7	Robert et al. (2016)
15.7	328	41	2	Daiyan et al. (2011)

3.1.2. Medium Sand

The unit weight of medium sand was categorized as ranging from 16 kN/m^3 to 16.7 kN/m^3. For this section, Trautmann and O'Rourke (1983), Karimian (2006), and Li (2016) data were used. The collection process for each test was significant different. The raw experimental data was acquired from Trautmann and O'Rourke (1983) and Li (2016),

while the data obtained from Karimian (2006) was digitized, however, their experimental approach was similar.

Karimian (2006) performed fourteen horizontal lateral pulling tests. The experimental test box was 2.5 m x 3.8 and provided a depth up to 2 m. The tests provided by Karimian (2006) included two types; pipes in medium sand and trenched pipes in medium sand. Karimian (2006) performed fourteen tests, however, only six tests were used because one test had an Hc/D = 1 and the others were trenched or used a geotextile liner.

Trautmann and O'Rourke (1983) used a pipe pulling method on eight medium sands. The test box was 1.2 m x 2.3 m x 1.2 m. The soils were spread in lifts and compacted in 100 mm sections. Displacement (mm) was measured by using a camera and a glass window for viewing. To increase the visibility of movement, flour was spread over each lift after compaction. By fitting a load cell at each end of a steel tie rod, which connected the jacking frame to the pipe axes, allowed for measurements of force (Trautmann and O'Rourke, 1983).

The tests data provided by Li (2016)Li (2016) was not accompanied with a publication written in English. Therefore, specifics of the experimental test was not able to be discussed in this section.

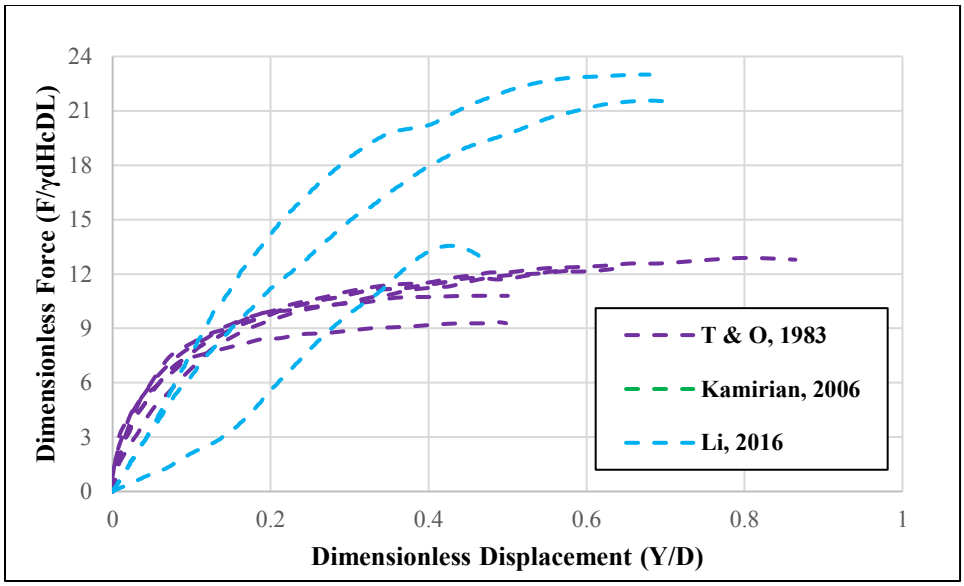

Figure 3-3: Medium sand data collection from various researchers, γ_d with a range of 16 kN/m^3 to 16.7 kN/m^3.

Data shown in Figure 3-3 encompassed these three researchers; totaling eighteen experiments. Table 3-2 describes the specific parameter from each researcher used in the construction of Figure 3-3. As stated previously, this research used a depth of Hc to normalize the force and facilitate the comparison of various tests. Trautmann and O'Rourke (1983), however, used H for force normalization. Never the less, the raw numerical-data was available for Trautmann and O'Rourke (1983) and Li (2016), the digitization and back calculation process was not needed. This was not the case for Kamiran (2006), and thus digitization was required.

Table 3-2: The parameters used for each test, described as medium sand, with the corresponding researcher.

γ_d (kN/m^3)	Length (mm)	Diameter (mm)	Hc/D	Experiment
16	2400	457	1.92	Karimian, (2006)
16	2400	457	1.92	Karimian, (2006)
16	2400	324	1.92	Karimian, (2006)
16	2400	324	1.92	Karimian, (2006)
16	2400	324	1.92	Karimian, (2006)
16	2400	324	2.75	Karimian, (2006)
16	1000	60	3	Li (2016)
16	1000	60	5	Li (2016)
16	1000	60	8	Li (2016)
16	1000	60	10	Li (2016)
16.4	1200	102	3.5	Trautmann and O'Rourke (1983)
16.4	1200	102	3.5	Trautmann and O'Rourke (1983)
16.4	1200	102	3.5	Trautmann and O'Rourke (1983)
16.4	1200	102	3.5	Trautmann and O'Rourke (1983)
16.4	1200	102	5.5	Trautmann and O'Rourke (1983)
16.4	1200	102	8	Trautmann and O'Rourke (1983)
16.4	1200	102	11	Trautmann and O'Rourke (1983)
16.4	1200	102	11	Trautmann and O'Rourke (1983)

3.1.3. Dense Sand

The third category was sand described as dense sand. The dry unit weight for dense sand is between 16.7 kN/m^3 to 17.5 kN/m^3. Figure 3-4 shows dimensionless force-displacement relationship for lateral pipe movement and is composed of data from four research groups; Hsu (1993), Turner (2004), Olson (2009), and Li (2016). This graph was created, by the use of fifteen experiments from the various researchers mentioned above.

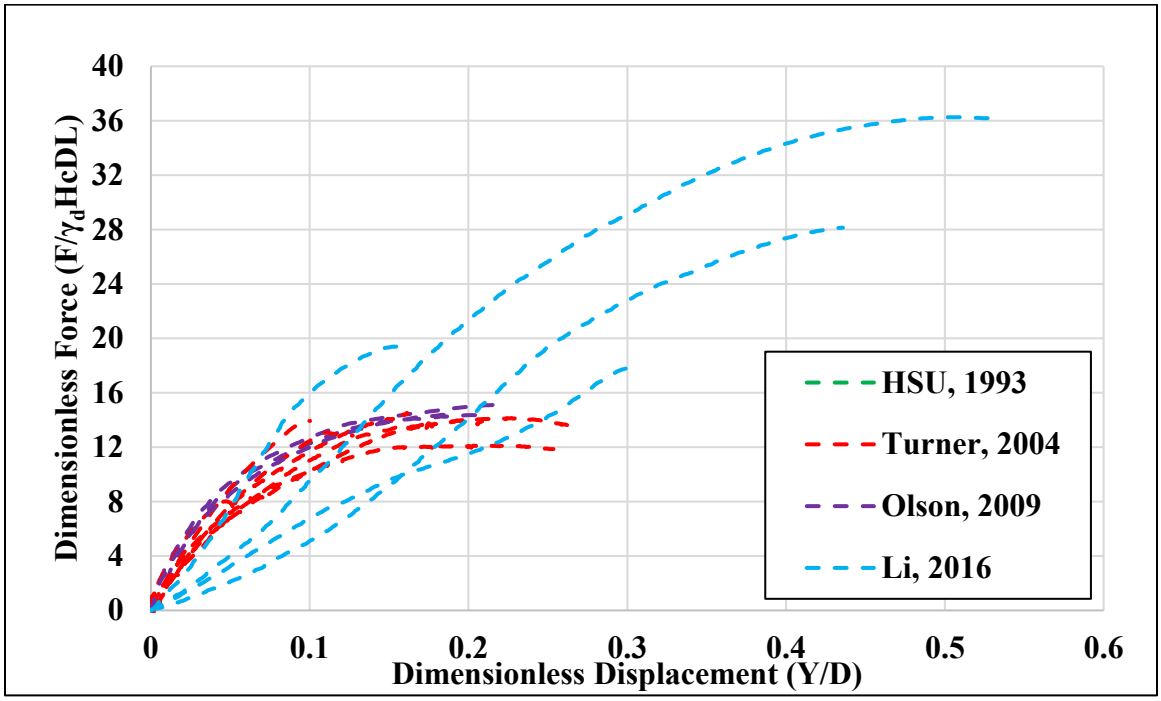

Figure 3-4: Dimensionless force vs. dimensionless displacement representation of dense sand ranging from γ_d = 16.7 kN/m^3 to 17.5 kN/m^3.

Refer to the pervious section discussing loose sand to understand how the Hsu (1993) tests were performed. Olson (2009) used two different test boxes. One box had an inner length of 2.44 m and one test was accomplished this way; with a pipe length of 2.44 m, D is 120 mm, and Hc = 0.63 m. While the other test box had an inner length of 1.6 m. Two test were performed using an Hc = 0.63 m, D = 124 mm, and L = 2.44 m. The unit weight for these three test varied from 16.9 kN/m^3 to 17.1 kN/m^3. Turner (2004) conducted six experiments, where the box dimensions were 1.6 m x 0.36 m x 0.36 m. Six tests were performed with similar independent variables; D = 120 mm, Hc = 0.65 m, and L = 1.21 m; However, the unit weight varied from 16.9 kN/m^3 to 17.2 kN/m^3. As mentioned previously, Li (2016) data was published in Chinese and an English description was not

available. Therefore, details of the experiment were not provided. As of 2018 summer, Jinlong Li and his research group is currently working on their paper to be published in English.

The original test data were not available for Hsu (1993), and the data needed to be manually digitized from the figure presented in Hsu (1993); which were overlapping at various points. This issue caused some difficulty in the data collection process. For Olson (2009), Turner (2004), and Li (2016), raw test data were available and used in the figure. The majority of the data presented in the graph follow a general trend, while the Li (2016) has a higher maximum dimensionless force when compared to the other researcher's data. Refer to Table 3-3 for the parametric values used in creating the Figure 3-4.

Table 3-3: Experiment from individual researchers describing the parameters used for dense sand.

γ_d (kN/m^3)	Length (mm)	Diameter (mm)	Hc/D	Experiment
16.9	2440	120	5.47	Olson (2009)
16.9	1210	120	5.5	Turner (2004)
17	1000	60	3	Li (2016)
17	1000	60	5	Li (2016)
17	1000	60	8	Li (2016)
17	1000	60	10	Li (2016)
17	1210	120	5.5	Turner (2004)
17.1	2440	124	5.29	Olson (2009)
17.1	1210	120	5.5	Turner (2004)
17.2	1200	76.2	2	Hsu (1993)
17.2	1200	76.2	4	Hsu (1993)
17.2	1200	76.2	6	Hsu (1993)
17.2	1200	76.2	8	Hsu (1993)
17.2	1200	76.2	10	Hsu (1993)
17.2	2440	124	5.29	Olson (2009)
17.2	1210	120	5.5	Turner (2004)
17.2	1210	120	5.5	Turner (2004)
17.2	1210	120	5.5	Turner (2004)

3.1.4. Very Dense Sand

Very dense soils were described as having a γ_d > 17.5 kN/m^3. The test results for these soils are displayed in Figure 3-5 below. To the best of this author's knowledge, the only available experiments on very dense sand were that performed by Trautmann and O'Rourke (1983). Refer to section 3.1.2., to understand how the tests were conducted and recorded by Trautmann and O'Rourke (1983). As shown in the Figure 3-5, the maximum displacement increases as a function of depth (Hc/D) (Trautmann and O'Rourke, 1983).

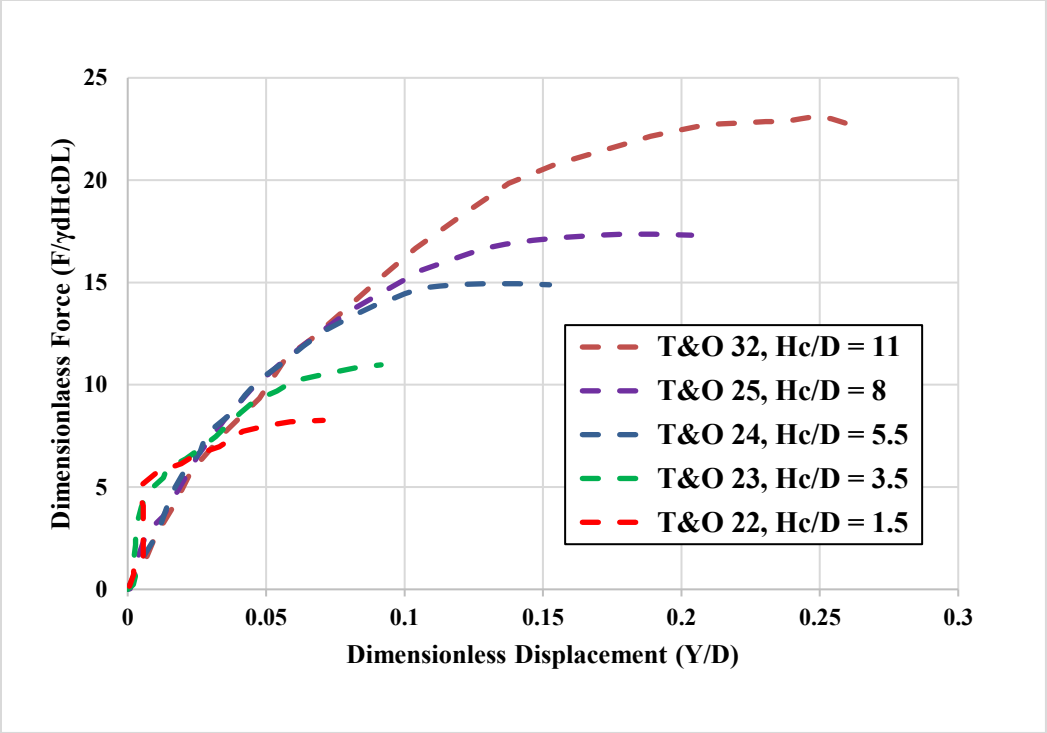

Figure 3-5: The dimensionless force vs. dimensionless displacement for very dense sand ($\gamma_d > 17.5$ kN/m^3)

Please note that the figure above does not represent the entire test experiment recorded by Trautmann and O'Rourke (1983). The data points exceeding F_{max} were neglected (refer to Figure 3-1). Only one of the five data sets, shown in Figure 3-5, was digitized. This data set is Hc/D = 1.5. The initial linear line of test 22 does not fit the general trend of the other test data and this difference can be associated with the digitization process. Table 3-4 is a summary of the different variables for each test. The unit weight of the soil, length, and diameter all remained constant, while Hc/D varied.

Table 3-4: Trautmann and O'Rourke (1983) very dense sand tests with varying Hc/D

γd (kN/m3)	Length (mm)	Diameter (mm)	Hc/D	Experiment
17.7	1200	120	1.5	Trautmann and O'Rourke (1983)
17.7	1200	120	3.5	Trautmann and O'Rourke (1983)
17.7	1200	120	5.5	Trautmann and O'Rourke (1983)
17.7	1200	120	8	Trautmann and O'Rourke (1983)
17.7	1200	120	11	Trautmann and O'Rourke (1983)

3.2. Data Calculation

To begin performing the data calculation process, an intermediate step was needed. This step involved finding the maximum dimensionless force (F'_{max}) with the corresponding maximum dimensionless displacement (Y'_{max}), as described by Jung et al. (2016). The maximum corresponding value was located; where a clear pick can be seen in the force vs. displacement graph or in a dimensionless graph (refer to Figure 3-1). Jung et al. (2013a and 2013b) described how a clear pick could be seen in the data provided by Trautmann and O'Rourke (1983), Turner (2004), and Olson (2009).

However, in some cases, especially for loose and medium sand, a definitive pick was not visible. In such cases, a different methodology or approach is required to define F'_{max}. Yimsiri et al. (2004) and Jung et al. (2013a and 2013b) describes how the maximum values can be selected, where a pick could not be seen (Figure 3-6).

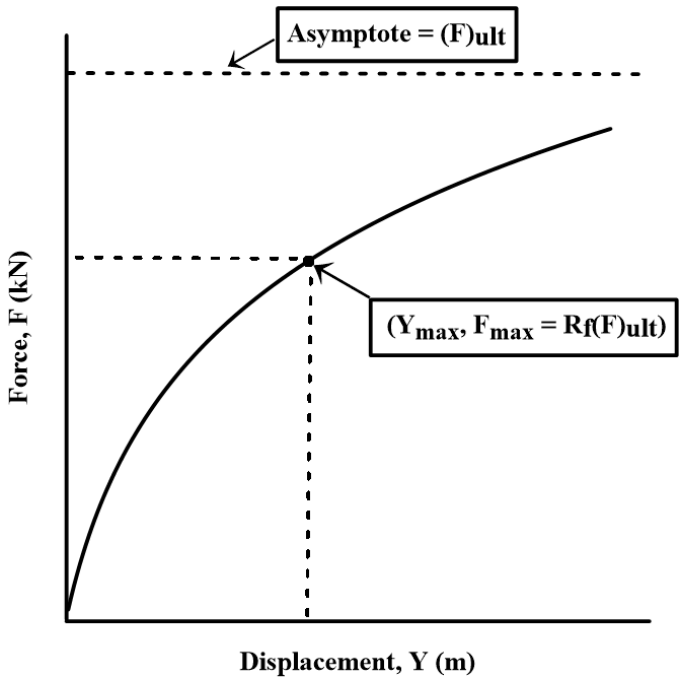

Figure 3-6: Determining F_{max} and Y_{max} for experimental data; not exhibiting a clear pick.

In Figure 3-6, Y is the displacement, $(F)_{ult}$ is the asymptotic value of the principal force difference, which the force vs. displacement curve approaches at the infinite displacement. As shown in Figure 3-6, the hyperbola remains below $(F)_{ult}$ within all finite values of displacement. The force difference at the maximum lateral pipe force, $(F)_{max}$, is expressed as:

$$R_f = \frac{F_{max}}{(F)_{ult}} \tag{3.1}$$

Duncan (1980) explains how the over estimation of maximum force is typically in the range of 11% on average, therefore a reduction factor (R_f) was needed to correct this over estimation. Wang and Duncan (1974) reported that R_f typically range between 0.5 to 0.9 for most soils. They also reported that the compressive strength of the soils is always less

than $(F)_{ult}$. By extrapolation, the hyperbolic curve was followed to find the location of $(F)_{ult}$ or the asymptote. $(F)_{ult}$ was then multiplied by a reduction factor of 0.9. The value found from this multiplication process is considered as F_{max}, Reference Appendix A: Table A-1 for corresponding values of each experiment. This research used a similar approach followed by Yimsiri et al. (2004) and Jung et al. (2013a and 2013b), $F_{max} = R_f (1/\beta)$, where $R_f = 0.9$, which is in agreement with the information used by Trautmann and O'Rourke (1985) and fall in the range of R_f reported by Wang and Duncan (1974).

The approach described by Yimsiri et al. (2004) and Jung et al. (2013a and 2013b) was developed from the method discussed and used by Hansen (1963), Duncan (1980), Fellenius (1980), and Trautmann and O'Rourke (1983). Similar approach were used in this study and are as follows:

When a clear pick was not visible, a hyperbolic curve was fitted from the obtained force (F)–displacement (Y) data by means of maximum force (F_{max}) extrapolation, using a similar approach noted by Trautmann and O'Rourke (1983) for characterizing the force–displacement relationship. As mentioned previously, the following hyperbola was fitted from the force–displacement relationship:

$$F = \frac{Y}{\alpha + \beta Y} \tag{3.2}$$

where $1/\alpha = \lim_{Y \to 0} (dF/dY)$ = initial force–displacement stiffness curve; and $(F)_{ult} = 1/\beta = \lim_{Y \to \infty} (F)$ = maximum force (F_{max}), (Yimsiri et al., 2004). The methodology described above is needed to locate the maximum force where a clear pick could not be seen.

After completion of the above step for each experiment following this trend, the normalization process of dimensionless force vs. dimensionless displacement could occur. The normalization process allowed each soil type to be presented in one of the two different ways as follows:

3.2.1. Single-Normalization

The hyperbolic stress-strain relationship was first developed by Kondner (1963) and further discussed and used by Wong and Duncan (1974) and Trautmann and O'Rourke (1983). Kondner (1963) describes how stress-strain curves for many soils can be accurately approximate by the hyperbola shown in Figure 3-7.

In 1974, Wong and Duncan developed a report explaining the hyperbolic relationship, the methodology used for finding the hyperbolic parameters, and how these parametric values are characterized for various soil types that relate to the stress-strain curve. The authors would like the readers to note that stress-strain relationships differ from force-displacement, however, they correlate to each other.

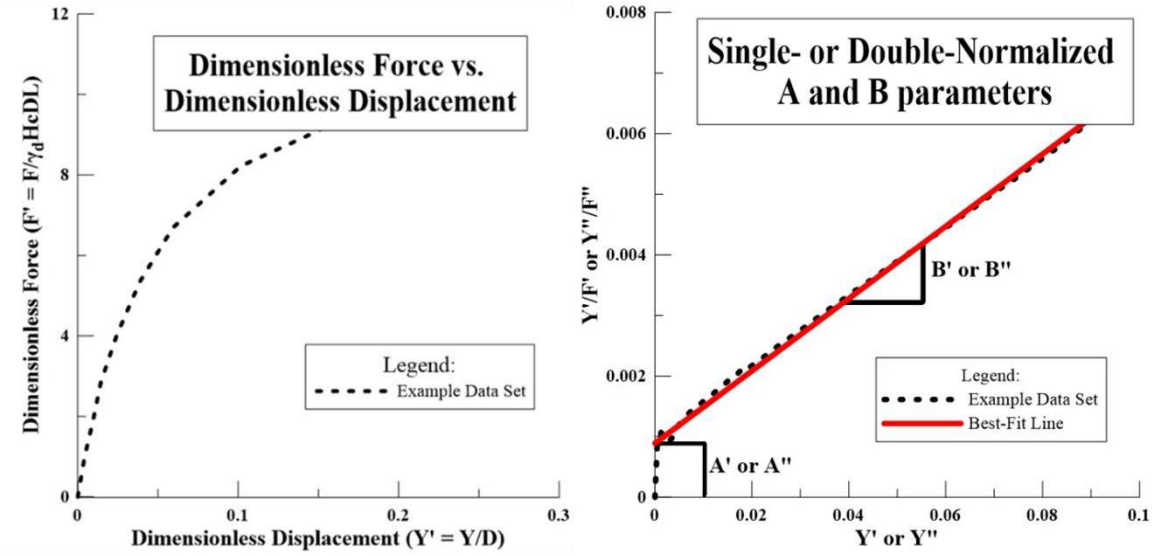

Figure 3-7: An example of a Dimensionless Force vs. Displacement (left image), and a Linear representation emphasizing A' or A" and B' or B" parameter produced be single- and double-normalization of dimensionless data set (right image).

First, the dimensionless force vs. dimensionless displacement were fitted and plotted on a transformed axis, Y'/F' and Y' as illustrated in Figure 3-7, where:

$$Y' = \frac{\mathrm{Y}}{\mathrm{D}} \tag{3.3}$$

$$F' = \frac{F}{\gamma_d HcDL} \tag{3.4}$$

Each parameter used in Eqs. 3.3 and 3.4 are defined previously. By plotting linearizing the dimensionless force vs. displacement on a transformed axis, the hyperbolic curve can be represented by a linear line, following the rectangular hyperbola:

$$F' = \frac{Y'}{B' + A'Y'} \tag{3.5}$$

The parameters describing the hyperbolic equation have a physical significance and are shown in Figure 3-7 and Equation 3.5, labeled as A' and B'. The A' parameter is similar to the initial tangential modulus, while the B' parameter relates to the asymptotic value

F_{ult} of the stress difference, discussed in the previous section (Wang and Duncan, 1974). This description is similar to the approach reported by Duncan and Chang (1970) and Trautmann and O'Rourke (1985).

The single-normalization process allows the data to be represented linearly on the transformed axis plot. This line is then fitted with a linear best-fit line. Furthermore, the best-fit line will represent the best-fit hyperbola (Duncan and Wong, 1974). Figure 3-7 was generated for each test data, by plotting the dimensionless force and displacement on a transformed axis. As shown in Figure 3-7, the line has two key values needed for this research. The A' and B' parameters for every test, previously mentioned, were found and recorded. The A' parameter is considered as the y-intercept, while B' is considered as the slope of the best-fit line. The research reported by Duncan and Chang (1970) and Trautmann and O'Rourke (1985) focused their attention on double-normalization, however, single precedes the double-normalization process.

3.2.2. Double-Normalization

After single-normalization occurred, the hyperbolic curve was then converted to a double-normalized force-displacement graph, by plotting on a transformed axis Y"/F" and Y" (Figure 3-7, right), as described by Kondner (1963), where:

$$F" = \frac{F'}{F'_{max}} \tag{3.6}$$

$$Y" = \frac{Y'}{Y'_{max}} \tag{3.7}$$

The double-normalization process followed a similar approach in finding the A" and B" parameter, as described by the Single-Normalization rectangular hyperbola (Equation 3.5), with the main differences being the hyperbolic equation, mentioned by Jung (2016):

$$F" = \frac{Y''}{B"+A"Y''}$$

(3.8)

As discussed in the previous section, the A" and B" parameter are the y-intercept and the slope, respectively. Again, these values were generated from the linear best-fit line, representing the hyperbolic curve, described by the double-normalization process (Eq. 3.8).

Equations 3.3 through 3.5 are similar to equations 3.6 through 3.8, with the maximum values, F'_{max} and Y'_{max}, playing an influential part in the double-normalization process. While, the single-normalization does not take into account the maximum force or displacement.

3.2.3. Outliers

After the A and B parameters were generated for each data set, the outliers were identified using the commercial statistical program, R 3.4.3. The A and B parameters for single- and double-normalization for each experiment, based on soil type, were inputted individually and a box plot was generated. A box-and-whisker plot is a graphical representation of the data as shown in Figure 3-8. The distance between upper (Q3) and lower quartile (Q1) is the inter quartile range (IQR). This range is classified as 50% of

the results. The minimum and maximum values are considered as the upper and lower whisker, however, if these values exceed 1.5 IQR they are deemed outliers. These outliers are further classified as mild or extreme; >1.5 IQR and > 3.0 IQR, respectively (Dienes, 2011).

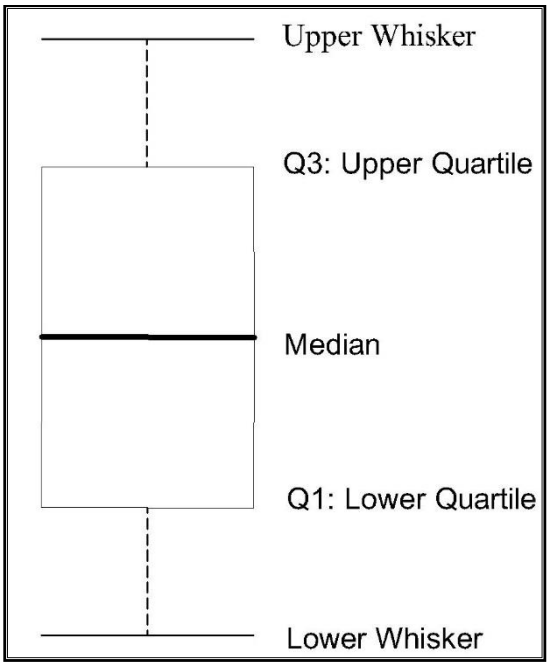

Figure 3-8: An example of a box-and-whisker plot.

During this procedure, if an A' or A" and B' or B" parameters for single- or double-normalization were found to be greater than 1.5 IQR, then the whole experiment was neglected and considered an outlier. Furthermore, this increased the overall accuracy of the results.

Chapter 4. Results and Discussion

4.1. Overview

This chapter includes a systematic arrangement of the results based on soil type; loose, medium, dense, and very dense, the outliers found in each test, and the A or B parameter for single-or double-normalization. The following single- and double-normalized graphs plotted on a transformed axis will emphasize all of the experiments performed by each respective researcher, however, a graph was generated for every data. An example of one experiment performed by each researcher is mentioned in Appendix A Figures A-1 through A-11.

4.1.1. Loose Sand

Figure 4-1 shows twenty-one experiments, performed by Burnett (2015), Almahakeri et al. (2013), Daiyan et al. (2011), Hsu (1993), and Robert et al. (2016), using a transformed axis to linearize the data with a 90% confidence interval (C.I.). For loose sand, none of the experimental data collected were considered as outliers by the box-and-whisker plot. As shown in Figure 4-1, the data plotted on the transformed axis follows a linear trend, with a different colored line, highlighting the experimental data performed by each researcher. The 90% C.I. is relative low and does not encompass many of the data sets. This occurrence is attributed to the lines with a relatively low y-intercept, which is pulling the overall average down. A linear line was fitted to each graph to find the A and B parameters for both single- and double-normalized transformed axis graphs.

The A and B parameters found from the linear fit line for each researcher is summarized in Table 4-1. The unit weight of the soil ranges from 14.6 kN/m^3 to 15.7 kN/m^3. The A' parameter for single-normalized Almahakeri et al. (2013), Hc/D = 7 with a γ_d = 15 kN/m^3 is 0.0294, which is similar to Hsu (1993), Hc/D = 8 with a γ_d = 15.2 kN/m^3, with an A' parameter of 0.0297. In regards to the same experiment, the B' parameters are significantly different. Almahakeri et al. (2013) B parameter is 0.0422 and Hsu (1993) is 0.0876. Similar trends were also found in double-normalization where the A" parameter were similar, however, the B" parameter was significantly different. Please refer to Table 4-1 for more detail.

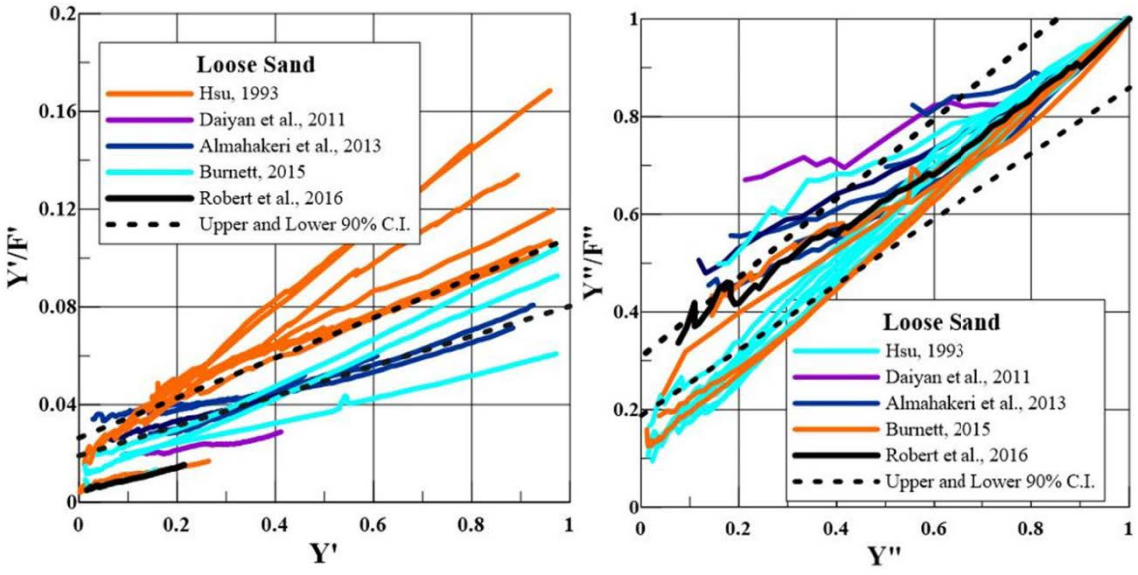

Figure 4-1: Compiled data from each respective researcher, plotted on a transformed axis, illustrating singe- (left) and double- (right) normalization with 90% C.I.

As found in Table 4-1, the A" parameter for double-normalization of Robert et al. (2016) is 0.3029, and the B" parameter is 0.6698. Robert et al. (2016) experiment had an Hc/D = 5.7 and γ_d = 15.3 kN/m^3. These results compare well with the results found from Alamhakeri et al. (2013), Hc/D = 7, with an A" = 0.3065 and B" = 0.6416. Again, by focusing on the double-normalization parameters, Burrnet (2015), where Hc/D is 3 and the γ_d = 14.6kN/m^3, had a very similar results when compared to Hsu (1993), where Hc/D = 4 and γ = 15.2 kN/m^3. In these two cases, the A' is 0.1006 and A" is 0.1015, and the B' is 0.9020 and B" is 0.9025, respectively.

Table 4-1: The parameters describing the linear fit of each data set based upon single- and double-normalization

γd (kN/m^3)	Hc/D	Single-Normalized		Double-Normalized		Experiment
		A'	B'	A"	B"	
14.6	3	0.0091	0.0858	0.1006	0.9020	Burnett (2015)
14.7	3	0.0123	0.0916	0.1168	0.8656	Burnett (2015)
14.8	7	0.0147	0.0469	0.2416	0.7492	Burnett (2015)
15	3	0.0192	0.0509	0.6177	0.3411	Almahakeri et al. (2013)
15	3	0.0154	0.0729	0.3164	0.6178	Almahakeri et al. (2013)
15	5	0.0256	0.0535	0.4014	0.5756	Almahakeri et al. (2013)
15	5	0.022	0.0545	0.4194	0.5427	Almahakeri et al. (2013)
15	7	0.0294	0.0422	0.4088	0.5321	Almahakeri et al. (2013)
15	7	0.0246	0.0557	0.3065	0.6416	Almahakeri et al. (2013)
15.2	2	0.0143	0.1621	0.0843	0.9258	Hsu (1993)
15.2	4	0.0305	0.0990	0.1015	0.9025	Hsu (1993)
15.2	6	0.0334	0.0968	0.1218	0.8715	Hsu (1993)
15.2	8	0.0297	0.0876	0.1074	0.9208	Hsu (1993)
15.2	10	0.0288	0.0821	0.0994	0.8963	Hsu (1993)
15.2	12	0.0317	0.0767	0.109	0.9328	Hsu (1993)
15.2	14	0.0323	0.074	0.1236	0.9083	Hsu (1993)
15.2	16	0.0308	0.0752	0.1203	0.9400	Hsu (1993)
15.2	20	0.0454	0.0711	0.1737	0.8786	Hsu (1993)
15.3	5.7	0.0098	0.0475	0.3029	0.6698	Robert et al. (2016)
15.4	3	0.0044	0.0512	0.3300	0.5970	Burnett (2015)
15.7	2	0.0168	0.0252	0.5806	0.3581	Daiyan et al. (2011)

Table 4-2 includes a summary of the overall range of the A' or A" and B' or B" parameters for each normalization process. From the data collected, the A' parameter ranges from 0.0044 to 0.0323 and B' ranges from 0.0252 to 0.1621 for single-normalization. The maximum value of A' parameter for single-normalization, from Y'/F'

vs. Y' graph, was determined from Hsu (1993), where Hc/D = 20 and γd = 15.2 kN/m^3. The minimum value from Burrnet (2015), where Hc/D = 3 and γ_d = 15.4 kN/m^3. The B' maximum (0.1621) and minimum (0.0252) represented data from Hsu (1993), where Hc/D = 2 and Daiyan et al. (2011), where Hc/D = 2, respectively.

Table 4-2: Maximum and minimum values of A and B parameter for single- and double-normalization

Parameter	Single-Normalized		Double-Normalized	
	A'	B'	A"	B"
Maximum	0.0454	0.1621	0.6177	0.9400
Minimum	0.0044	0.0252	0.0843	0.3411

For double-normalization, the A" parameter ranged from 0.0843 to 0.6177 and B" parameter ranged from 0.3411 to 0.9400. Of these four values obtained, the data provided by Almahakeri et al. (2013), Hc/D = 3 and γ_d = 15 kN/m^3, described the maximum A" parameter and the minimum B" parameter. While, for the ranges previously mentioned, the parameters found from Hsu (1993), Hc/D = 2, described the minimum A", while Hsu (1993), Hc/D = 16, defines the maximum B".

4.1.2. Medium Sand

Initially, eighteen tests were used in this experiment. Of those eighteen experiments, four were found to be outliers, by use of the box-and-whisker method. These four tests, deemed as outliers, were from Li (2016) provided data. The fourteen tests had a soil unit weight varying from 16 kN/m^3 to 16.4 kN/m^3. The single- and double-normalized graphs

are displayed in Figure 4-2, representing experiments from two researchers (Trautmann and O'Rourke, 1983 and Karimian, 2006).

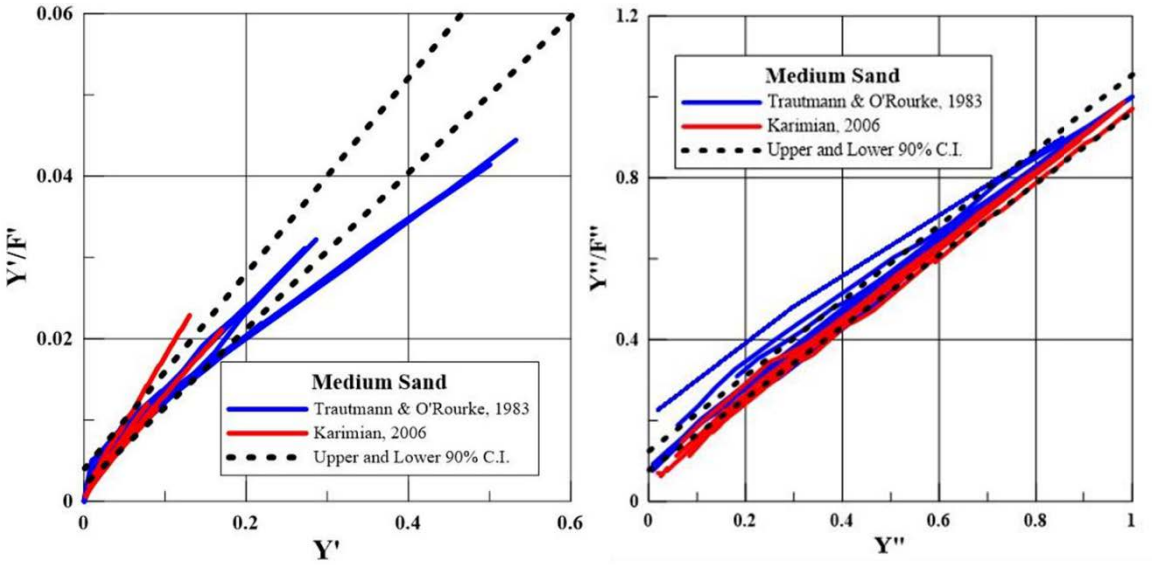

Figure 4-2: Compiled data without outliers from each respective researcher, plotted on a transformed axis, illustrating singe- (left) and double- (right) normalization with 90% C.I.

The left image, single-normalization, appears to show the data beginning at the origin. This is due to the values of the y-intercept (A' parameter) being relatively small. The majority of the tests fall within the 90% confidence interval. The A-parameter is larger for the double-normalized, providing greater visibility in the plot. All of the experiments, shown in the figure above, exhibit a linear trend. By the nature of each normalization process, the maximum dimensionless displacement (Y') and maximum Y'/F' varies for each individual experiment in the single-normalized graph, while double-normalization process forces the maximum Y"/F" and maximum Y" to be 1. The occurrence for the maximum value to be (1,1) is because of the calculation process for double-

normalization. As mentioned previously, each experiment shown in Figure 4-2 were generated separately. The A' or A" and B' or B" parameters found from each graph are presented in Table 4-3.

The A' parameter for single normalization, describing Karimian (2006), ranges from 0.0005 to 0.0014 with a γ_d = 16 kN/m^3 and Hc/D varying from 1.92 to 2.75. The five tests performed by Karimian (2006) include a B' parameter bounded between 0.1137 and 0.1659. Trautmann and O'Rourke (1983) had a slightly higher A' parameter ($0.002 \leq A \leq 0.0074$) and a smaller B' parameter ($0.0701 \leq B \leq 0.1065$), however, the γ_d was 16.4 kN/m^3 and the Hc/D ranged from 3.5 to 11. When comparing the two researcher's data separately, the A' and B' parameters for single-normalization did not overlap, yet, this occurrence did not happen with the double normalization case.

Table 4-3: The parameters, without outliers, describing the linear fit of each data set based upon single- and double- normalization

γ_d (kN/m^3)	Hc/D	Single-Normalized		Double-Normalized		Experiment
		A'	B'	A"	B"	
16	1.92	0.0014	0.1168	0.0761	0.928	Karimian, (2006)
16	1.92	0.0011	0.1137	0.1007	0.893	Karimian, (2006)
16	1.92	0.0005	0.1299	0.0482	0.9548	Karimian, (2006)
16	1.92	0.0007	0.1433	0.0631	0.9356	Karimian, (2006)
16	1.92	0.0006	0.131	0.066	0.9474	Karimian, (2006)
16	2.75	0.0013	0.1659	0.0541	0.9181	Karimian, (2006)
16.4	3.5	0.0026	0.1065	0.0697	0.9623	Trautmann and O'Rourke (1983)
16.4	3.5	0.002	0.1048	0.0629	0.946	Trautmann and O'Rourke (1983)
16.4	3.5	0.0034	0.1049	0.1583	0.8883	Trautmann and O'Rourke (1983)
16.4	3.5	0.0037	0.1021	0.154	0.8544	Trautmann and O'Rourke (1983)
16.4	5.5	0.0036	0.0838	0.1464	0.8641	Trautmann and O'Rourke (1983)
16.4	8	0.0045	0.0743	0.0846	0.9385	Trautmann and O'Rourke (1983)
16.4	11	0.0074	0.0701	0.2236	0.7753	Trautmann and O'Rourke (1983)
16.4	11	0.0053	0.0737	0.1016	0.9103	Trautmann and O'Rourke (1983)

The double-normalization process allowed for each researcher, regardless of the independent variable (e.g., γ_d, Hc/D) to be well distributed. For example, the A" parameters for Trautmann and O'Rourke (1983) were distributed between 0.0629 to 0.2236 and the B" between 0.7753 to 0.9623. The range of A" and B" parameters from Karimian (2006) were similar to Trautmann and O'Rourke (1983); namely, 0.0482 to 0.10007 and 0.8930 to 0.9548.

Table 4-4 describes the maximum and minimum values resulting from the experimental normalization method of medium sands. The single-normalized A' parameters are less than the double-normalized, this is also the case for B' parameter. These differences in A and B parameters are inherently visible in Figure 4-2.

Table 4-4: Maximum and minimum values for medium sand

Parameter	Single Normalized		Double Normalized	
	A'	B'	A"	B"
Maximum	0.0179	0.1659	0.3857	0.9623
Minimum	0.0005	0.0701	0.0482	0.7532

4.1.3. Dense Sand

The data collected, classified as dense soil, totaled eighteen tests from four researchers (Hsu, 1993; Turner,2004; Olson,2009; and Jinlong Li,2016). Of these eighteen test, four tests were found to be possible outliers by the use of the box-and-whiskers plot method. Three of the four tests, provided Li (2016), were considered as outlier, as well as, one test from Hsu (1993), where Hc/D = 10.

Fourteen tests are represented in Figure 4-3. Both the single- and double-normalization graphs, plotted on a transformed axis, display a linear trend for almost all of the experimental data. By using the transformed axis method this allows for the hyperbolic line to be represented in a linear fashion. The majority of the tests fall within the range of the 90% C.I for single-normalization, accept for Li's (2016). Even though, experiment

labeled as Li, 2016 followed a concave trend, instead of linear, a portion of this test was excluded (red dashed line in Figure 4-3). This occurrence was most likely due to improper compaction of the soil during the initial setup of the test in the test box. The linear portion, with a positive slope, was used in finding the A and B parameters. The right image, in Figure 4-3, the included portion falls within the bounds of the other experimental data and within the 90% confidence interval.

Most of the data in Figure 4-3 have a smooth linear trend (e.g., Turner, 2004 and Olson, 2009), while Hsu (1993) is jagged. The distinction between these two types of lines reflects the data collection process. The Hsu (1993) data was digitized from the graph presented in the paper, while the other researcher's data was the original, performed in each test.

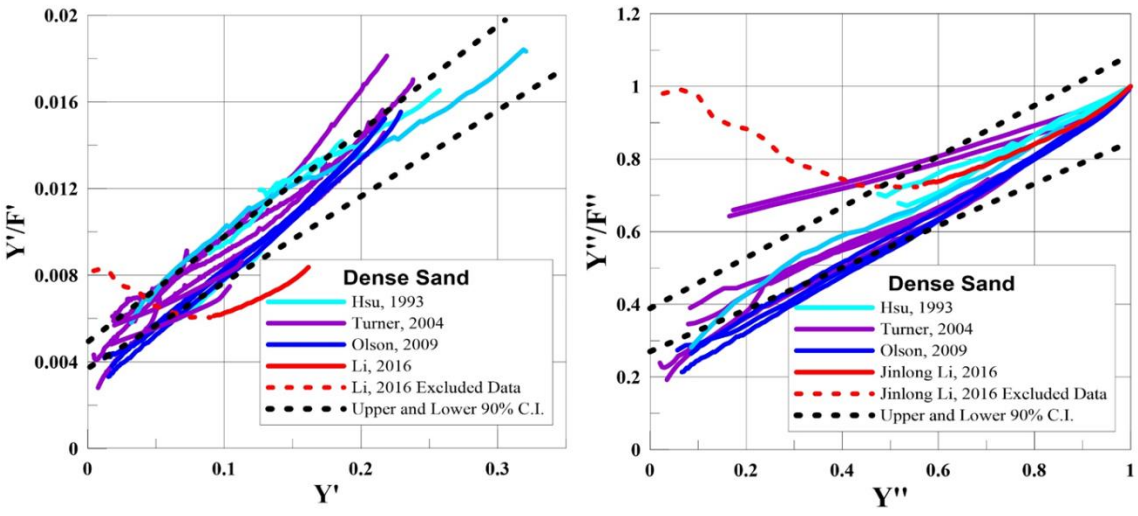

Figure 4-3: Single- (left image) and double-normalization (right image), described as dense, plotted on a transformed axis without outliers with 90% C.I.

Table 4-5 , summarizes the entire A' or A" and B' or B" parameters for the different graphs described as single- and double-normalization in Figure 4-3. The dry unit weight of the soil was confined between 16.9 kN/m^3 and 17.2 kN/m^3. The Hc/D for each experiment varied from 2 to 8. The A and B parameters were well distributed, meaning that none of the researchers were bounded by the upper or lower portion of each parameter.

Table 4-5: Represents the A and B parameters found from each of the two transformed normalization graphs with respect to dense sand

γd (kN/m^3)	Hc/D	Single-Normalized		Double-Normalized		Experiment
		A'	B'	A"	B"	
16.9	5.47	0.0029	0.0532	0.2036	0.7644	Olson (2009)
16.9	5.5	0.0034	0.0490	0.1902	0.8060	Turner (2004)
17	3	0.0032	0.0297	0.3550	0.6141	Li (2016)
17	5.5	0.0049	0.0310	0.5714	0.4030	Turner (2004)
17.1	5.29	0.0030	0.0519	0.1976	0.7582	Olson (2009)
17.1	5.5	0.0051	0.0416	0.3835	0.6020	Turner (2004)
17.16	2	0.0037	0.0543	0.3579	0.6335	Hsu (1993)
17.16	4	0.0055	0.0442	0.4113	0.5305	Hsu (1993)
17.16	6	0.0073	0.0352	0.4365	0.5458	Hsu (1993)
17.16	8	0.0053	0.0407	0.2594	0.7385	Hsu (1993)
17.2	5.29	0.0024	0.0539	0.1596	0.7956	Olson (2009)
17.2	5.5	0.0042	0.0264	0.5650	0.3814	Turner (2004)
17.2	5.5	0.0049	0.0464	0.3070	0.6245	Turner (2004)
17.2	5.5	0.0038	0.0610	0.2130	0.7296	Turner (2004)

Below, Table 4-6 describes the maximum values for the A and B parameters. For single-normalization, the A' parameter was approximately 0.0024 to 0.0073 and the B 'parameter was 0.0264 to 0.0610. The double-normalization parameter were significantly higher, with A" being within a range of 0.1596 and 0.5714 and B" bounded by 0.3814 to 0.8060.

Table 4-6: The upper and lower bounds of the A and B parameters

Parameter	Single-Normalized		Double-Normalized	
	A'	B'	A"	B"
Maximum	0.0073	0.0610	0.5714	0.8060
Minimum	0.0024	0.0264	0.1596	0.3814

4.1.4. Very Dense Sand

The fourth and final classification of soil is defined as very dense with a $\gamma_d \geq 17.5$ kN/m^3. Five test were found from Trautmann and O'Rourke (1983) and are shown in Figure 4-4. The left graph, relating to single-normalization, is spread-out until a dimensionless displacement ≤ 0.075. In the right image, the test data converge to a linear line at (1,1).

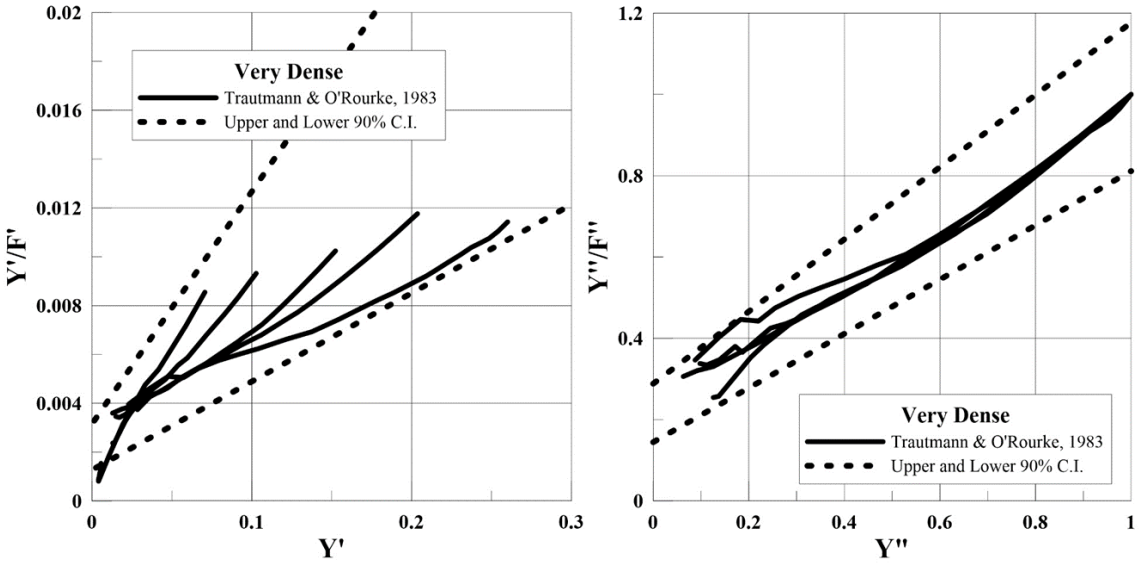

Figure 4-4: Single- (left image) and double-normalization (right image), described as very dense, plotted on a transformed axis with 90% C.I.

The data sets for both single- and double-normalization fall within the confidence interval, with a small portion of a test, Hc/D =1.5, falling outside. This occurrence can be attributed to the data collection process used; digitized. The single-normalization C.I. spreads out as the F'/Y" and Y' increase. This widening of the interval is due to the data sets covering a wider range as Y'/F' and Y'.

Table 4-7 mentioned below describes each of the four tests shown in Figure 4-4, where the γ_d remained constant and the Hc/D varied from 1.5 to 11. As Hc/D increases, for both single- and double-normalization, the A" parameter increases, while the B" parameter decreases.

Table 4-7: Represents the A and B parameters found from each of the two transformed normalization graphs with respect to very dense sand

γd (kN/m^3)	Hc/D	Single-Normalized		Double-Normalized		Experiment
		A’	B’	A”	B”	
17.7	1.5	0.0008	0.1112	0.1024	0.9020	Trautmann and O'Rourke (1983)
17.7	3.5	0.0011	0.0810	0.1344	0.8972	Trautmann and O'Rourke (1983)
17.7	5.5	0.0025	0.0447	0.2512	0.666	Trautmann and O'Rourke (1983)
17.7	8	0.0026	0.0412	0.2410	0.6891	Trautmann and O'Rourke (1983)
17.7	11	0.0034	0.0285	0.2975	0.6497	Trautmann and O'Rourke (1983)

Table 4-8 below illustrate the ranges of the A and B parameters, regardless the Hc/D. The single-normalization A’ parameter are between 0.0008 and 0.0034, while for double-normalization A” flocculates from 0.1344 to 0.2975. The B’ parameter, for single, is from 0.0285 to 0.1112 and 0.6497 to 0.9020 for double, respectively.

Table 4-8: Minimum and Maximum A and B parameters for very dense sand

Parameter	Single-Normalized		Double-Normalized	
	A’	B’	A”	B”
Maximum	0.0034	0.1112	0.2975	0.9020
Minimum	0.0008	0.0285	0.1024	0.6497

4.2. Compiled Data

Fifty-four tests are shown in Figure 4-5, of which, twenty-one were described as loose, fourteen medium and dense, and five very dense sand. The slope of line (B’ parameter)

increases as the unit weight decreases for single-normalization. The A' parameter shows a different trend with A' increasing in order from medium to very dense and dense to loose sand.

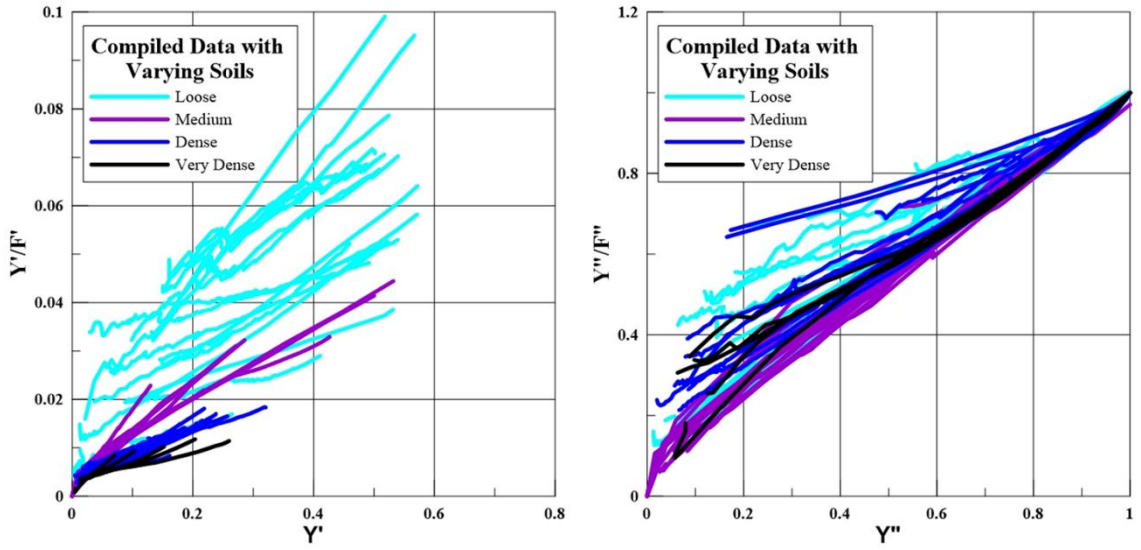

Figure 4-5: Compiled data for single- (left image) and double-normalization (right image) with varying soil unit weight.

The right plot in Figure 4-5 shows the liner line extended to (1, 1). This (1,1) maximum value correlates directly the process associated with the double-normalization process. The A" parameter is increasing in sequential order from medium to loose and dense to very dense sand. Individual loose sand experiments are sporadic throughout the graphs. This is also exemplified in Figure 4-6 for single-normalization, where the grouping of loose sand is minimal. Medium sand has a higher B' parameter when compared to the other soils. As unit weight increases, the B' parameter decreases, however, the A' parameter remains relatively the same. The correlation between A' and B' changed significantly with respect to double-normalization.

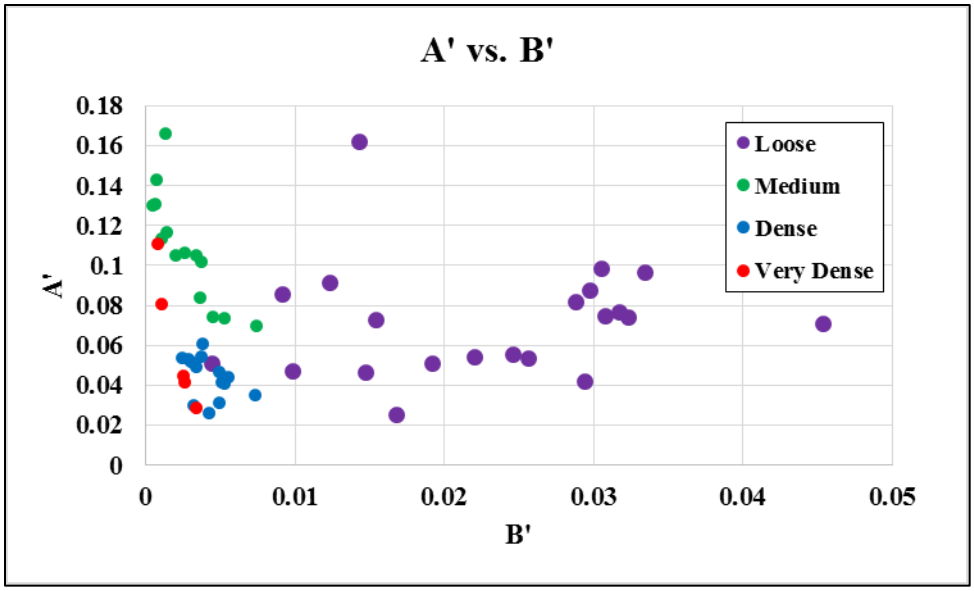

Figure 4-6: Single-normalization of A' plotted against B' parameter.

The A" and B" parameter for double-normalization, plotted on the x- and y-axis, respectively, are shown in Figure 4-7. All of the data points found exhibit a linear-trend, even though the unit weight varied for each experiment. A linear regression line Y = -1.1401X+ 1.0178 with a high r^2 (0.97) correlates A" and B" parameters by the negative slopped line. Again, data points in blue (loose sand) have the highest range (distance between maximum and minimum) of A" and B" parameters, followed by dense sands (grey). Mediums sands (orange) B" parameter range was less than very dense sands (yellow), while the A" parameter was slightly greater.

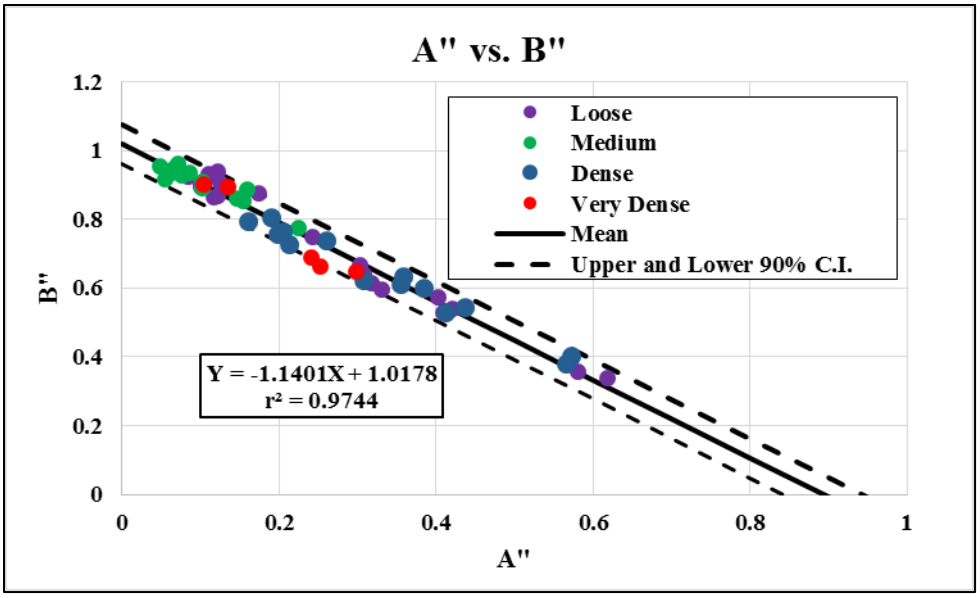

Figure 4-7: Double-normalization of A" plotted against B" parameter with 90% C.I.

The information previously described is summarized in Table 4-9 below. The average A' parameter for single-normalization is as follows: very dense (0.0021), dense (0.0043), medium (0.0027), and loose (0.0229). For all soil types, the average B' parameter is bounded by 0.0442 to 0.1086, and the corresponding values with in this range are shown below, as well. With respect to double-normalization, the A" parameter for loose, medium, dense, and very dense are 0.2468, 0.1007, 0.3294, and 0.2053, respectively. 0.7413, 0.9083, 0.6377, and 0.7608 are the average B" parameter for soils ranging from 14.6 kN/m^3 to 17.7 kN/m^3.

Table 4-9: Average A and B parameters for each soil type

		Average			
		Single-Normalized		Double-Normalized	
	Parameter	A’	B’	A”	B”
Soil Type	Loose	0.0229	0.0715	0.2468	0.7413
	Medium	0.0027	0.1086	0.1007	0.9083
	Dense	0.0043	0.0442	0.3294	0.6377
	Very Dense	0.0021	0.0613	0.2053	0.7608

The average double-normalized A” and B” parameter for loose soil, reported by Trautmann and O’Rourke (1983), was 0.15 and 0.85, while the results found in this study were 0.2468 and 0.7413, respectively. This difference can be attributed to the number of data sets collected when compared with the number of tests performed by Trautmann and O’Rourke (1983). The parameters found, in this research, for loose sand are more generalized. Lastly, the tests, performed by Trautmann and O’Rourke (1983), describing loose sand were not used in this research because the author used Trautmann and O’Rourke (1983) for comparison. The author was interested in finding the variability in the result mentioned by Trautmann and O’Rourke (1983) and found in this research. Lastly, Trautmann and O’Rourke (1983) did not provide the recorded data for loose sand. For medium sand, Trautmann and O’Rourke (1983) reported the A” and B” parameters for double-normalization as 0.1 and 0.9, respectively, which were in agreement with the values found in this research 0.1007 and 0.9083, respectively. Trautmann and O’Rourke (1983), however, did not mention parameters for dense soils. The result reported by Trautmann and O’Rourke (1983) for very dense sand were as follows, for A” and B” parameter, 0.25 and 0.75. In this study, by using the same test data performed by

Trautmann and O'Rourke (1983) were slightly different with 0.2053 and 0.7608, respectively.

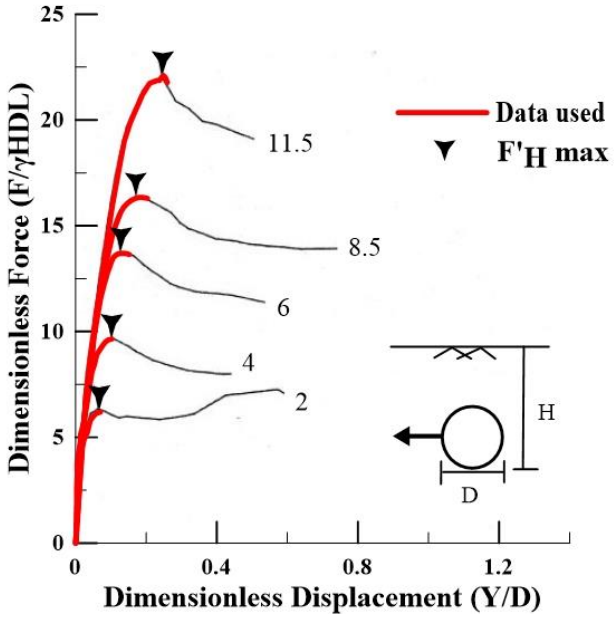

Figure 4-8: Data used for very dense sand and compared with F'_H max provided by Trautmann and O'Rourke, 1983.

These differences, mentioned previously, can be attributed to the maximum force chosen, when compared with the values selected by Trautmann and O'Rourke (1983), refer to Figure 4-8. The termination of the red line was the F'_{max} for this research. Lastly, the data for H/D = 2 (Hc = 1.5) was digitized, which may have introduces some unintended error.

Chapter 5. Summary, Conclusion, and Future Work

5.1. Summary

The need to secure resources, such as water and oil, is becoming a cause of concern for inhabitants all around the world. Pipes below subsurface, especially those crossing a fault boundary, are susceptible to permanent ground deformation. A force-displacement behavior study was conducted on four types of soil; loose, medium, dense, and very dense sands. This study focused on experiments, performed by ten researchers, involving $H_c/D \geq 1.5$, where the A and B parameters for single- and double-normalization, plotted on a transformed axis, were investigated.

An extensive literature review was designated to understand how the tests were conducted, what types of tests were suitable for this case study, and how the parameters would be found. Soil-pipe interaction, are typically categorized as axial, lateral, or vertical; described by the bearing directions. This research was tailored towards plane strain lateral loading. Also, the approach for finding the various A and B parameters were detailed in the methods portion.

A detailed analysis of the A and B parameters were investigated. The average, maximum, and minimum values for each soil type were found. The values were then compared with the results produced by Trautmann and O'Rourke in 1983.

5.2. Conclusion

After a detailed literature review and an extensive data collection process, the average, minimum, and maximum A and B parameter were found for all respective soil types, ranging from loose to very dense sands. The A" parameter for double-normalization were 0.2053 for very dense, 0.3294 for dense, 0.1007 for medium, and 0.2619 for loose sands. While, the B" parameters were 0.7608 for very dense, 0.6377 for dense, 0.9083 for medium, and 0.7257 for loose sands. For validation, F'_{max}, chosen in this research, was compared with the F'_{max} selected by Trautmann and O'Rourke (1983) for very dense sands. The F'_{max} selected corresponded well with the F'_{max} values provided by Trautmann and O'Rourke (1983). Lastly, the results found by Trautmann and O'Rourke (1983), regarding A and B parameters, were in agreement with the parameters found in this research for loose, medium, and very dense sand. It was noted that the relative dimensionless-depth was taken as $Hc/D \geq 1.5$.

By plotting the A' vs. B', for single-normalization a correlation was not visible, however, this was not the case for double-normalization. The A" vs. B" graph showed a negative linear relationship with a coefficient of determinants. This relationship has never been described before, which suggests there is a correlation between the two parameters. By finding this correlation it allowed for the model to become more simplistic. Before, an individual would need to find both the A" and B" parameters. Now, by using this plot, only one unknown is needed. By finding one unknown, instead of two, decrease the length of the calculation process. By finding A" and B", it is possible to back calculate and create hyperbolic curve that represents the experimental values, which is comparative

to the field condition where a pipe is positioned perpendicular to a slope. This model is applicable in the designing process of a pipe positioned in such a manner.

The variety of test from different researchers allows for a wide range of soils to be represented. This allows for the A and B parameters to be generalized. Due to this generalization, this study can help field engineers to decide what types of soils are needed to combat failures associated with permeant ground deformation. Lastly, by understanding what type of pipe is needed, based upon the factor of safety, can decrease the overall cost of a project related to over designing.

5.3. Limitation of the study

This report is a systematic review study. The data was collected from other researchers within this field of study. Some of the data provided was from the original researcher, while others were digitized. If all of the data were of actual origin, meaning from each researcher, then a more accurate and representative result would follow; however, the original experimental data was not available from each individual researcher. Also, results could not be found from other researchers, describing the average double-normalized A" and B" parameters for dense sand. Therefore, the average A" and B" parameters for dense sand, found in this study, were not compared with other researchers. Lastly, more data sets may have been attained from other researchers, as well as, experimentation performed by the author. These limitations are most likely due to lack of funding and available resources.

5.4. Recommendations for future work

This research was focused on lateral pipe movement under plane-strain condition. However, a new study could investigate how the A and B parameters are affected in upward, downward, and oblique displacement within the confines of a pipe below subsurface, as well as, in a trenched system. After these parameters are found, an addition study could investigate how the A and B parameters change when the soils are interlaid with geotextiles. Additionally, it would be applicable to look at the A and B parameters for saturated soils which are more representative of field conditions. There is a need for more studies to understand how the A and B parameters are affected based upon the geotextile used, soil conditions, and displacement direction. By finding how these parameters are affected. The overall cost of project may decrease as a result of determining if pipes below subsurface are over designed.

The results found in this study could be compared with a finite element analysis model. This would give insight into how comparable the A and B parameters found in this study are with the model. Lastly, regression analysis or analysis of variance could be performed on the A and B parameters. The results from this analysis would useful to discern if there is a correlation between the A and B parameters with changes in the independent variables.

REFERENCES

ABAQUS (2017). "User's manual." ABAQUS, Inc., Providence, RI.

Almahakeri, M., Fam, A. and Moore, I.D., (2013). "Longitudinal bending and failure of GFRP pipes buried in dense sand under relative ground movement." *Journal of Composites for Construction*, *17*(5), pp. 702-710.

American Lifelines Alliance. (2005) "Seismic Design Guidelines for Water Pipelines" American Lifelines Alliance in partnership with the Federal Emergency Management Agency, Washington, D.C. www.americanlifelinesalliance.org

ASCE. (1984). "Guidelines for the Seismic Design of Oil and Gas Pipeline Systems.", Committee on Gas and Liquid Fuel Lifelines, American Society of Civil Engineers, Reston, Virginia, pp. 150-221

Audibert, J. M. E., and Nyman, K. J., (1975). "Coefficients of Subgrade Reaction for the Design of Buried Piping." Proceedings of the Second ASCE Specialty Conference on Structural Design of Nuclear Plant Facilities, held at New Orleans, La., vol. IA, Dec., pp. 109-141.

Audibert, J.M.E. and Nyman, K.J. (1977). "Soil Restraint Against Horizontal Motion of Pipes". Journal of the Geotechnical Engineering Division, ASCE, Vol. 103, No. GTlO, 1119-1142.

Burnett, A., (2015). "*Investigation of full scale horizontal pipe-soil interaction and large strain behaviour of sand*" (Doctoral dissertation).

Daiyan, N., Kenny, S., Phillips, R. and Popescu, R., (2011). "Investigating pipeline–soil interaction under axial–lateral relative movements in sand." *Canadian Geotechnical Journal*, *48*(11), pp. 1683-1695.

Das, B.M., Seeley, G.R. (1975) "Load displacement relationship for vertical anchor plates." Journal of Geotechnical Engineering Division, 101(GT7), pp.711-715.

Dienes, E. (2011), "Box Plot." <https://www.ctspedia.org/do/view/CTSpedia/CaseStudyPlot> (May 15, 2018).

Duncan, J.M. (1980). "Hyperbolic stress-strain relationships." Proceedings, Symposium on Limit Equilibrium, Plasticity and Generalized Stress-Station Applications in Geotechnical Engineering, held in conjunction with the 1980 ASCE Annual Convention and Exposition, Hollywood, FL, Oct. 27-31, 443–460.

Duncan, J.M., and Chang, C.Y. (1970). "Nonlinear Analysis of Stress and Strain in Soils." Journal of Soil Mechanics and Foundations, ASCE, Vol. 96, No. 5, Sep/Oct., 1629-1653.

Fellenius, B.H. (1980). "The Analysis of Results from Routine Pile Load Tests." Ground Engineering, Vol. 13, No. 6, 19–31.

Fern, J., Soga, K., and Robert, D.J. (2014a). "Shear strength and dilatancy of partially saturated sand in direct shear tests." *Proc., TC105 ISSMGE Int. Symp. on Geomechanics from Micro to Macro*, Taylor and Francis, London, pp. 1391-1396.

Fern, J., Soga, K., Robert, D.J., and Sakanoue, T. (2014b). "Shear strength and dilatancy of unsaturated silica sand in triaxial compression tests." *Proc., 14th Int. Conf. of Int. Association for Computer Methods and Recent Advances in Geomechanics,* Taylor and Francis, London, pp. 535-540.

Hansen J.B. (1953) “Earth pressure calculation: application of a new theory of rupture to the calculation and design of retaining walls, anchor slabs, free sheet walls, anchored sheet walls, fixed sheet walls, braced walls, double sheet walls and cellular cofferdams.” Danish Technical Press, Copenhagen., Denmark.

Hansen, J. B. (1961) “The Ultimate Resistance of Rigid Piles Against Transversal Forces,” Danish Geotechnical Institute (Geoteknisk Institut) Bull. Copenhagen, Vol. 12, 5-9.

Hansen, J.B. (1963). Discussion of “Hyperbolic Stress-Strain Response: Cohesive Soils.” by Kondner, R.L. Journal of the Soil Mechanics and Foundations Division, ASCE, Vol. 89, 299 No. SM4, 241 – 242.

Honegger, D. and Nyman, D.J. (2004). “Guidelines for the Seismic Design and Assessment of Natural Gas and Liquid Hydrocarbon Pipelines,” Pipeline Research Council International, Catalog No. L51927, October, pp. 563-570.

Hsu, T.W. (1993) “Rate effect on lateral soil restraint of pipeline.” Soils and Foundation, 33(4), 159-169.

Jung, J. K., O’Rourke, T. D., & Argyrou, C. (2016). “Multi-directional force–displacement response of underground pipe in sand”. Canadian Geotechnical Journal, (999), pp. 1-19.

Jung, J.K., O’Rourke, T.D., and Olson, N.A. (2013a). “Uplift Soil-Pipe Interaction in Granular Soil”, Canadian Geotechnical Journal, 50(7), pp. 744-753.

Jung, J.K., O’Rourke, T.D., and Olson, N.A. (2013b). “Lateral Soil-Pipe Interaction in Dry and Partially Saturated Sand”, J. Geotech. Geoenviron. Eng., 139(12), pp. 2028-2036.

Karimian, S.A. (2006), "Response of buried steel pipelines subjected to longitudinal and transverse ground movement." Ph.D. Thesis, University of British Columbia, Vancouver, B. C.

Konder, R.L., "Hyperbolic Stress-Strain Response: Cohesive Soils." Journal of the Soil Mechanics and Foundation Division, ASCE, Vol. 89, No. SM1, Feb., 1963, pp. 115-143

Kondner, R. L., & Zelasko, J. S. (1964). Void ratio effects on the hyperbolic stress-strain response of a sand. In *Laboratory shear testing of soils*. ASTM International.

Kostyukov, V.D. (1967) "Distribution of the density of sand in the sliding wedge ion front of anchor plates." Soil Mechanics and Foundation Engineering, 1, 12-13.

Li, J. (2016) "Research on lateral sand-pipe interaction". Master Thesis. Beijing University of Technology, Beijing, China

Neely, W.J., Stuart, J.G., and Graham, J. (1973). "Failure loads of vertical anchor plates in sand." Journal of Soil Mechanics Foundation Division, 99(9), 669-685.

Olson, N.A. (2009). "Soil Performance for Large Scale Soil-Pipeline Tests." Ph.D. Thesis, Cornell University, Ithaca, New York.

O'Rourke, T.D. (2010). "Geohazards and Large, Geographically Distributed Systems", Rankine 335 Lecture, Geotechnique, 60(7), pp. 505-543.

O'Rourke, T.D., Y. Wang, and P. Shi, (2004). "Advances in Lifeline Earthquake Engineering", 337 Keynote Paper, Proceedings, 13th World Conference on Earthquake Engineering, 338 Vancouver, B.C., Canada, Aug., Paper No. 5003

Oversen, N. K. (1964). “Anchor slabs, calculation methods, and model tests.” *Bulletin No. 16*, Danish Geotechnical Institute, Copenhagen, Denmark, 1-39.

Oversen, N.K., and Stromann, H. (1972). “Design Method for Vertical Anchor Slabs in Sand.” Proceedings, Specialty Conference on Performance of Earth and Earth-Supported Structures, ASCE, New York, Vol. 1, 1481-1500.

R Core Team, (2017). “A Language and Environment for Statistical Computing. R Core Team, R Foundation for Statistical Computing, Vienna, Austria. https://www.R-project.org/.

Robert, D.J. (2010). “Soil-pipeline interaction in unsaturated soils.” Ph.D. thesis, University of Cambridge, Cambridge, U.K.

Robert, D.J., and Soga, K. (2013). “Soile-pipeline interaction in unsaturated soils.” Chapter 13, *Mechanics on unsaturated geomaterials*, L. Laloui, ed., Wiley, London, pp. 303-325.

Robert, D.J., Soga, K., and O’Rourke, T.D. (2016). “Pipelines subjected to fault movement in dry and unsaturated soils.” *Int. J. Geomech.*, 10.1061/(ASCE)GM.1943-5622.0000548, C4016001.

Rowe, R.K., and Davis, E.H. (1982). “The behaviour of anchor plates in sand.” *Geotechnique*, 32(1), 25-41

Smith, J.E. (1962). “Deadman anchorages in sand.” Technical Report R199, U.S. Naval Civil Engineering Laboratory, Port Hueneme, CA.

Sokolovskii, V.V. (1965). “Statics of granular materials.” Pergamon Press, Oxford, London

Trautmann, C.H., and O'Rourke, T.D. (1983). "Behavior of Pipe in Dry Sand Under Lateral and Uplift Loading." Geotechnical Engineering Report 83-7, Cornell University, Ithaca, New York

Trautmann, C.H. and O'Rourke, T.D. (1985). "Lateral force-displacement response of buried pipe." Journal of Geotechnical Engineering, ASCE, 111(9): 1068-1084.

Trautmann, C.H., O'Rourke, T.D., and Kulhawy, F.H. (1985). "Uplift Force displacement Response of Buried Pipe." Journal of Geotechnical Engineering, Vol. 111, No. 9, pp. 1061-1076.

Turner, J.E., (2004). "Lateral Force – Displacement Behavior of Pipes in Partially Saturated Sand." M.S. Thesis, Cornell University, Ithaca, New York.

Wijewickreme, D., Karimian, H., and Honegger, D., (2009). "Response of buried steel pipelines subjected to relative axial soil movement." *Canadian Geotechnical Journal* 46.7 (2009): 735-752.

Wong, K.S., and Duncan, J.M. (1974). "Hyperbolic Stress-Strain Parameters for Nonlinear Finite 355 Element Analyses of Stresses of Stresses and Movements in Soil Masses." Report No. 356 TE-74-3, University of California, Department of Civil Engineering, Berkeley, California.

Yimisiri, S., Soga, K., Yoshizaki, K., Dasari, G.R., and O'Rourke, T.D. (2004). "Lateral and uplift soil-pipeline interactions in sand for deep embedment conditions." Journal of Geotechnical and Geoenvironmental Engineering, 130(8), 830-842.

APPENDENCES

Appendix A. A description of each test with the corresponding F_{max}, Y_{max}, and A and B parameter.

γd (kN/m^3)	Length (mm)	Diameter (mm)	Y_{max} (cm)	F_{max} (kN)	Hc/D	Single-Normalized		Double-Normalized		Experiment
						A'	B'	A"	B"	
14.6	914	254	24.75	27.19	3	0.0091	0.0858	0.1006	0.902	Burnett (2015)
14.7	914	254	24.69	24.37	3	0.0123	0.0916	0.1168	0.8656	Burnett (2015)
14.8	914	254	24.71	97.6	7	0.0147	0.0469	0.2416	0.7492	Burnett (2015)
15	1824	114	3.05	8.45	3	0.0192	0.0509	0.6177	0.3411	Almahakeri et al. (2013)
15	1840	115	5.28	9.6	3	0.0154	0.0729	0.3164	0.6178	Almahakeri et al. (2013)
15	1824	114	6.91	18.1	5	0.0256	0.0535	0.4014	0.5756	Almahakeri et al. (2013)
15	1840	115	6.02	18.05	5	0.022	0.0545	0.4194	0.5427	Almahakeri et al. (2013)
15	1824	114	10.09	30.87	7	0.0294	0.0422	0.4088	0.5321	Almahakeri et al. (2013)
15	1840	115	10.65	29.22	7	0.0246	0.0557	0.3065	0.6416	Almahakeri et al. (2013)
15.2	1200	38.1	3.71	0.3	2	0.0143	0.1621	0.0843	0.9258	Hsu (1993)
15.2	1200	38.1	7.01	0.77	4	0.0305	0.099	0.1015	0.9025	Hsu (1993)
15.2	1200	38.1	9.39	1.43	6	0.0334	0.0968	0.1218	0.8715	Hsu (1993)
15.2	1200	38.1	11.08	2.22	8	0.0297	0.0876	0.1074	0.9208	Hsu (1993)
15.2	1200	38.1	12.02	2.88	10	0.0288	0.0821	0.0994	0.8963	Hsu (1993)
15.2	1200	38.1	13.34	3.85	12	0.0317	0.0767	0.109	0.9328	Hsu (1993)

15.2	1200	38.1	12.21	4.55	14	0.0323	0.074	0.1236	0.9083	Hsu (1993)
15.2	1200	38.1	12.09	5.28	16	0.0308	0.0752	0.1203	0.94	Hsu (1993)
15.2	1200	38.1	11.66	6.39	20	0.0454	0.0711	0.1737	0.8768	Hsu (1993)
15.3	2030	114.6	2.45	15.78	5.7	0.0098	0.0475	0.3029	0.6698	Robert et al. (2016)
15.4	914	254	3.98	31.75	3	0.0044	0.0512	0.33	0.597	Burnett (2015)
15.7	328	41	1.68	0.25	2	0.0168	0.0252	0.5806	0.3581	Daiyan et al. (2011)
16	2400	457	7.79	123.76	1.92	0.0014	0.1168	0.0761	0.928	Karimian (2006)
16	2400	457	4.62	122.67	1.92	0.0011	0.1137	0.1007	0.893	Karimian (2006)
16	2400	324	2.81	45.96	1.92	0.0005	0.1299	0.0482	0.9548	Karimian (2006)
16	2400	324	2.84	51.05	1.92	0.0007	0.1433	0.0631	0.9356	Karimian (2006)
16	2400	324	2.21	80.39	1.92	0.0006	0.131	0.066	0.9474	Karimian (2006)
16	2400	324	4.21	62.91	2.75	0.0013	0.1659	0.0541	0.9181	Karimian (2006)
16.4	1200	102	3.38	6.52	3.5	0.0026	0.1065	0.0697	0.9623	Trautmann and O'Rourke (1983)
16.4	1200	102	1.59	5.83	3.5	0.002	0.1048	0.0629	0.946	Trautmann and O'Rourke (1983)
16.4	1200	102	2.07	6	3.5	0.0034	0.1049	0.1583	0.8883	Trautmann and O'Rourke (1983)
16.4	1200	102	3.44	6.47	3.5	0.0037	0.1021	0.154	0.8544	Trautmann and O'Rourke (1983)
16.4	1200	102	2.42	11.38	5.5	0.0036	0.0838	0.1464	0.8641	Trautmann and O'Rourke (1983)
16.4	1200	102	5.94	20.27	8	0.0045	0.0743	0.0846	0.9385	Trautmann and O'Rourke (1983)

16.4	1200	102	6.53	27.74	11	0.0074	0.0701	0.2236	0.7753	Trautmann and O'Rourke (1983)
16.4	1200	102	3.82	25	11	0.0053	0.0737	0.1016	0.9103	Trautmann and O'Rourke (1983)
16.9	2440	120	2.48	46.63	5.47	0.0029	0.0532	0.2036	0.7644	Olson (2009)
16.9	1210	120	2.6	24.11	5.5	0.0034	0.049	0.1902	0.806	Turner (2004)
17	1000	60	0.9	3.55	3	0.0032	0.0297	0.355	0.6141	Li (2016)
17	1210	120	1.35	21.25	5.5	0.0049	0.031	0.5714	0.403	Turner (2004)
17.1	2440	124	2.7	48.47	5.29	0.003	0.0519	0.1976	0.7582	Olson (2009)
17.1	1210	120	2.59	22.63	5.5	0.0051	0.0416	0.3835	0.602	Turner (2004)
17.16	1200	76.2	0.91	2.79	2	0.0037	0.0543	0.3579	0.6335	Hsu (1993)
17.16	1200	76.2	1.46	6.27	4	0.0055	0.0442	0.4113	0.5305	Hsu (1993)
17.16	1200	76.2	2.01	11.21	6	0.0073	0.0352	0.4365	0.5458	Hsu (1993)
17.16	1200	76.2	2.85	17.32	8	0.0053	0.0407	0.2594	0.7385	Hsu (1993)
17.2	2440	124	2.84	50.34	5.29	0.0024	0.0539	0.1596	0.7956	Olson (2009)
17.2	1210	120	1.25	22.9	5.5	0.0042	0.0264	0.565	0.3814	Turner (2004)
17.2	1210	120	2.85	23.04	5.5	0.0049	0.0464	0.307	0.6245	Turner (2004)
17.2	1210	120	2.62	19.91	5.5	0.0038	0.061	0.213	0.7296	Turner (2004)
17.7	1200	120	0.86	8.21	1.5	0.0008	0.1112	0.1024	0.902	Trautmann and O'Rourke (1983)
17.7	1200	120	1.05	8.53	3.5	0.0011	0.081	0.1344	0.8972	Trautmann and O'Rourke (1983)
17.7	1200	120	1.55	18.08	5.5	0.0025	0.0447	0.2512	0.666	Trautmann and O'Rourke (1983)

17.7	1200	120	2.08	30.61	8	0.0026	0.0412	0.241	0.6891	Trautmann and O'Rourke (1983)
17.7	1200	120	2.65	55.32	11	0.0034	0.0285	0.2975	0.6497	Trautmann and O'Rourke (1983)

Appendix B. An example graph, from each researcher, highlighting the A and B parameters for single- and double-normalization; described by unit weight

As described by the linear line in Figure A-1, single-normalized (left image), Y = 0.0469X + 0.0147, where A' is 0.0147, B' is 0.0469, determination coefficients of is 0.99. For the linear line provided by double-normalization (right image), Y = 0.7492X + 0.2416, A" parameter is 0.2416, B" is 0.7492, and determination of coefficients is 0.99.

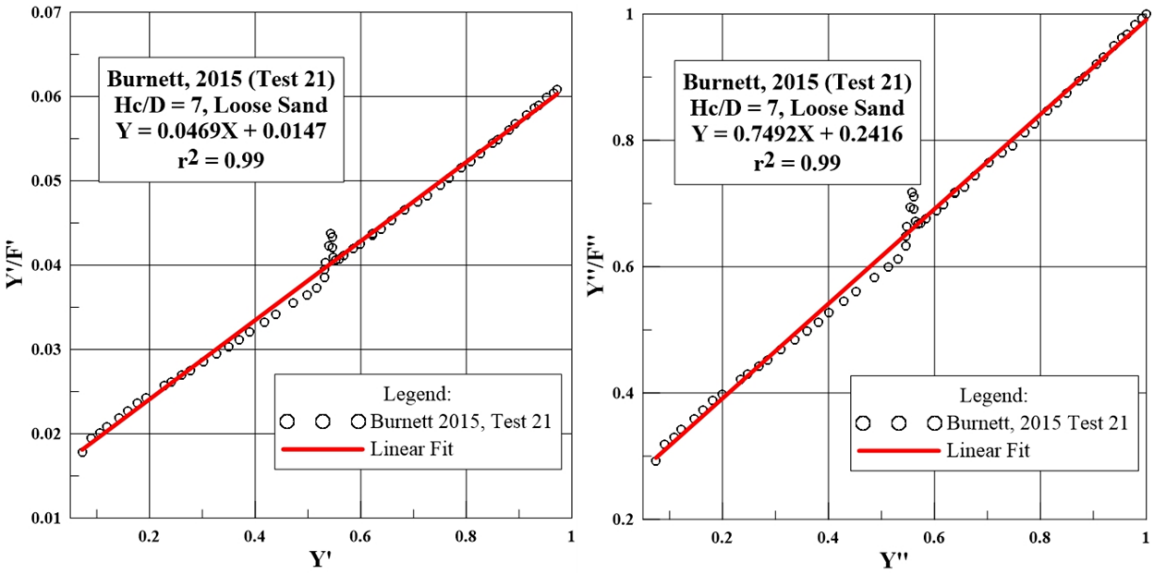

Figure B-1: Burnett (2015), Test 21, plotted on a single- (left) and double- (right) normalized transformed axis.

As described by the linear line in Figure A-2, single-normalized (left), Y = 0.0557X + 0.0246, where A' is 0.0246, B' is 0.0557, and determination of coefficients is 0.98. For the linear line provided by double-normalization (right image), Y = 0.6416X + 0.3065, A" parameter is 0.3065, B" is 0.6416, and determination of coefficients is 0.98.

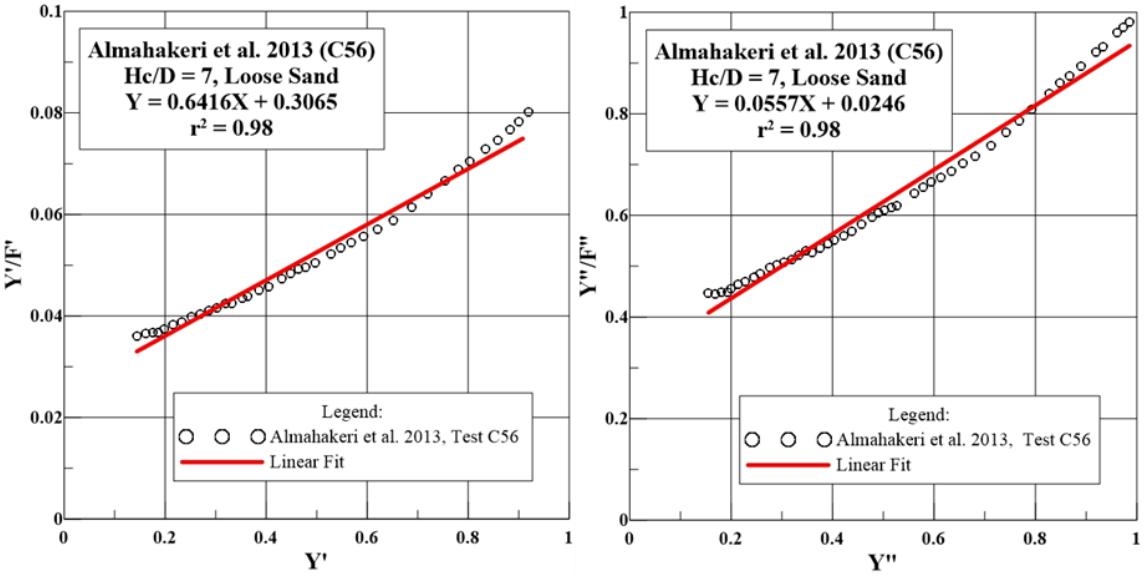

Figure B-2: Test C56 (Hc/D = 7) performed by Almahakeri et al. (2013) plotted on a transformed axis (single- (left) and double- (right) normalized).

As described by the linear line in Figure A-3, single-normalized (left image), Y = 0.0963X + 0.0098, where A' is 0.0098, B' is 0.0963, and determination of coefficients is 0.99. For the linear line provided by double-normalization (right image), Y = 0.6583X + 0.3115, A" parameter is 0.3115, B" is 0.6538, and determination of coefficients is 0.99.

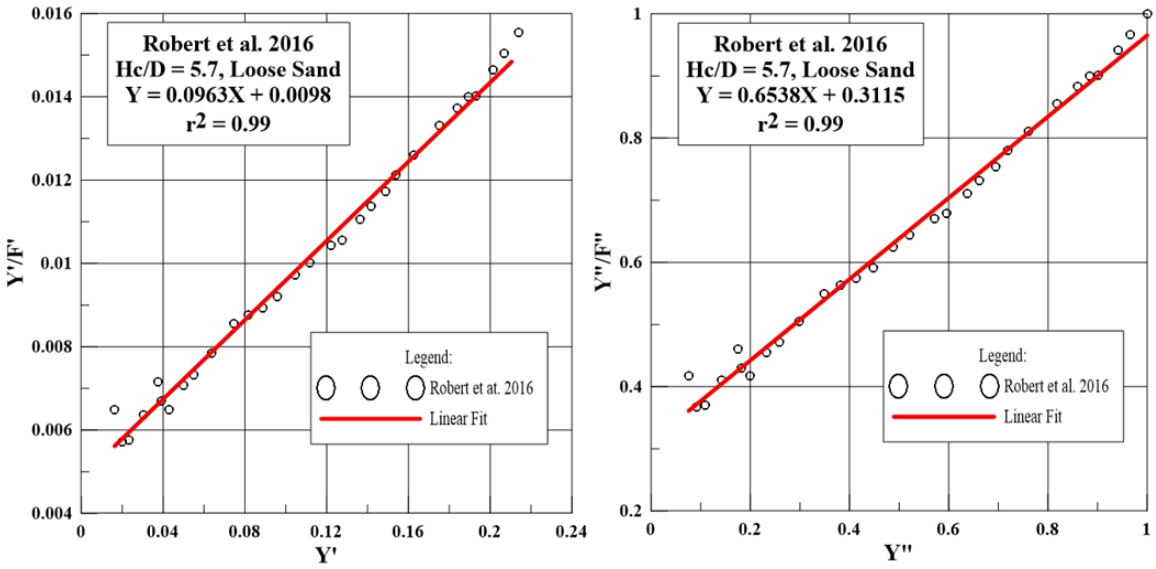

Figure B-3: Single- and double- normalized graph created by the experimental data provided by Robert et al. (2016).

As described by the linear line in Figure A-4, single-normalized (left image), Y = 0.00252X + 0.0168, where A' is 0.0168, B' is 0.0252, and determination of coefficients is 0.94. For the linear line provided by double-normalization (right image), Y = 0.3581X + 0.5806, A" parameter is 0.5806, B" is 0.3581, and determination of coefficients is 0.94.

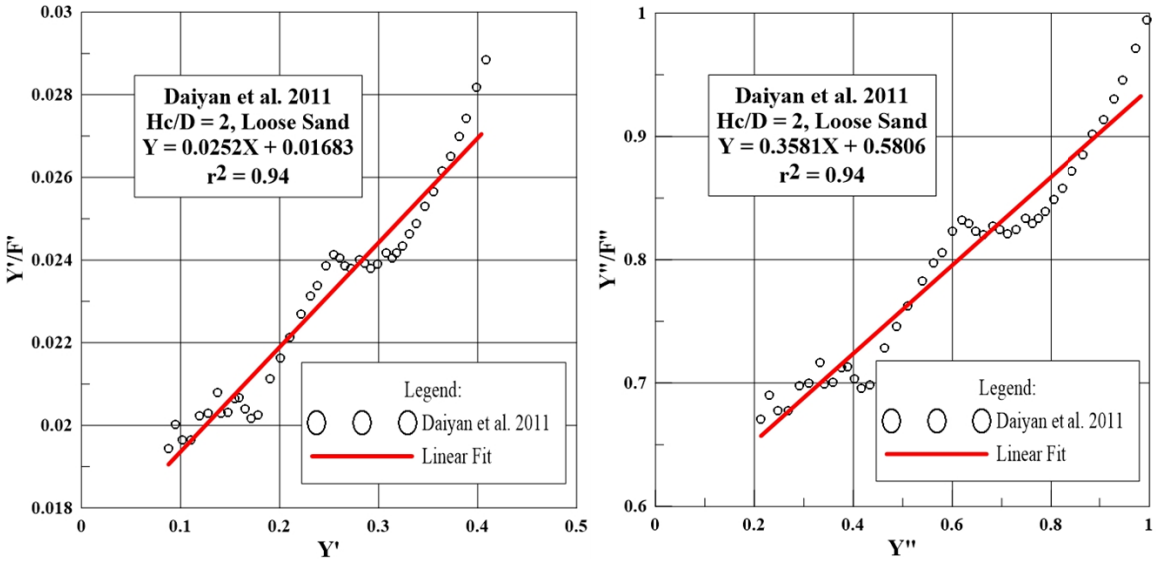

Figure B-4: Data provided from Daiyan et al. 2011 plotted on a transformed axis; single- (right) and double- (left) normalized.

As described by the linear line in Figure A-5, single-normalized (left image), Y = 0.0711X + 0.0454, where A' is 0.0454 and B' is 0.0711. For the linear line provided by double-normalization (right image), Y = 0.8786X + 0.1737, A" parameter is 0.1737 and B" is 0.8786.

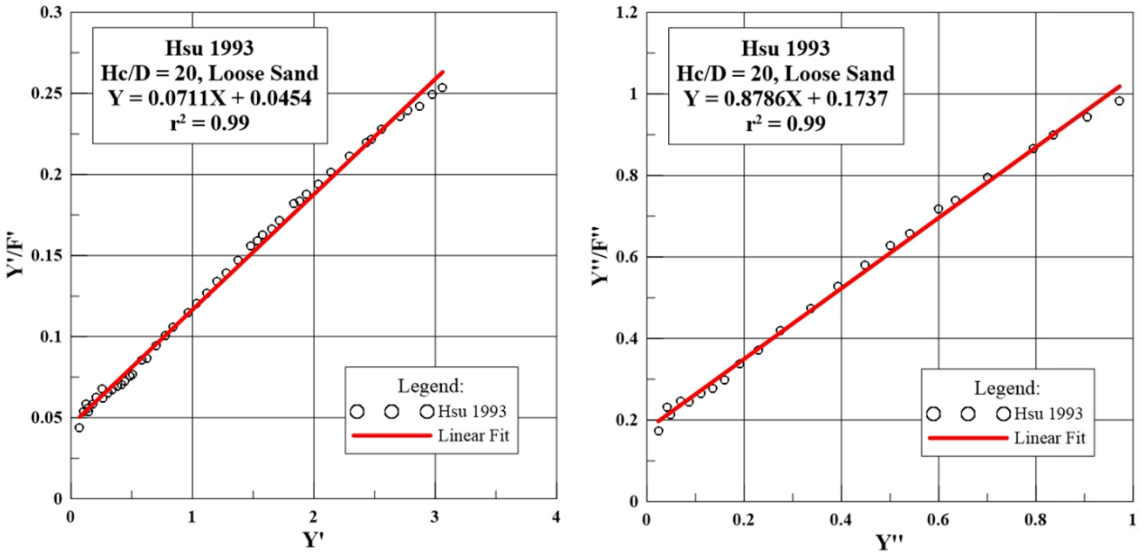

Figure B-5: Data provided from Hsu (1993) plotted on a transformed axis; single- (right) and double- (left) normalized.

As described by the linear line in Figure A-6, single-normalized (left image), Y = 0.1433X + 0.0007, where A' is 0.0007 and B' is 0.1433. For the linear line provided by double-normalization (right image), Y = 0.9356X + 0.0631, A" parameter is 0.0631 and B" is 0.9356.

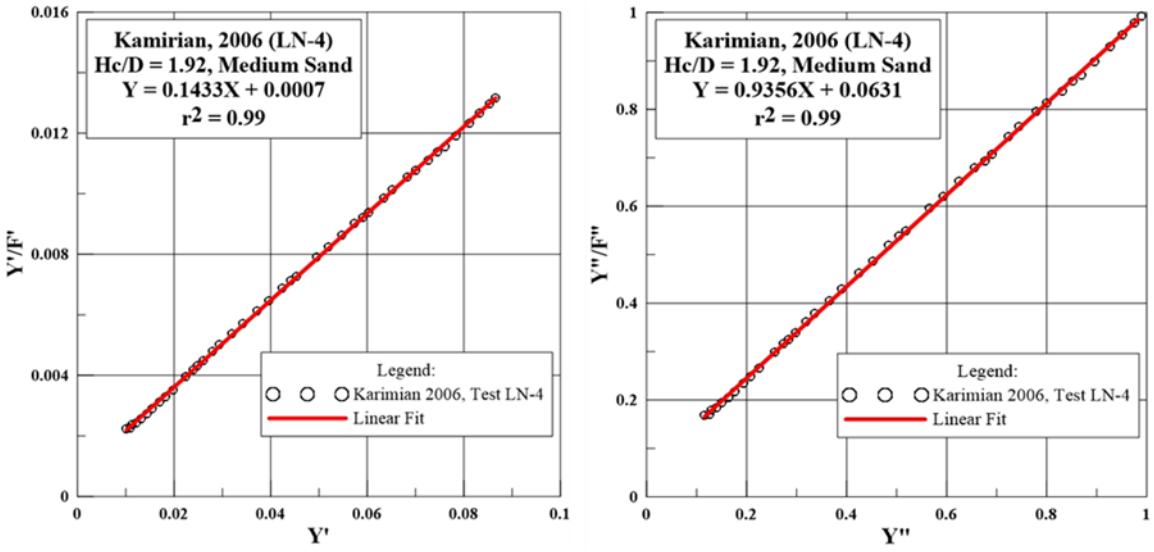

Figure B-6: Data provided from Karmian (2006) plotted on a transformed axis; single- (right) and double- (left) normalized.

As described by the linear line in Figure A-8, single-normalized (left image), Y = 0.1065X + 0.0026, where A' is 0.0026 and B' is 0.1065. For the linear line provided by double-normalization (right image), Y = 0.9623X + 0.0697, A" parameter is 0.0697 and B" is 0.9623.

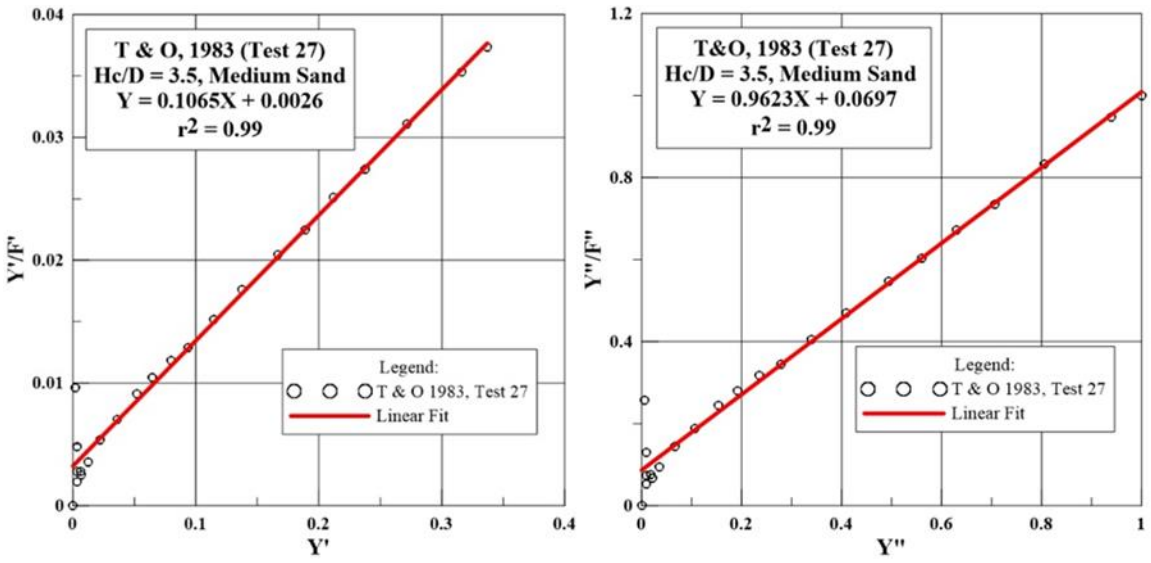

Figure B-7: Trautmann and O'Rourke (1983), Test 27, plotted on a single- (left) and double- (right) normalized transformed axis.

As described by the linear line in Figure A-9, single-normalized (left image), Y = 0.0532X + 0.0029, where A' is 0.0029 and B' is 0.0532. For the linear line provided by double-normalization (right image), Y = 0.7644X + 0.2036, A" parameter is 0.2036 and B" is 0.7644.

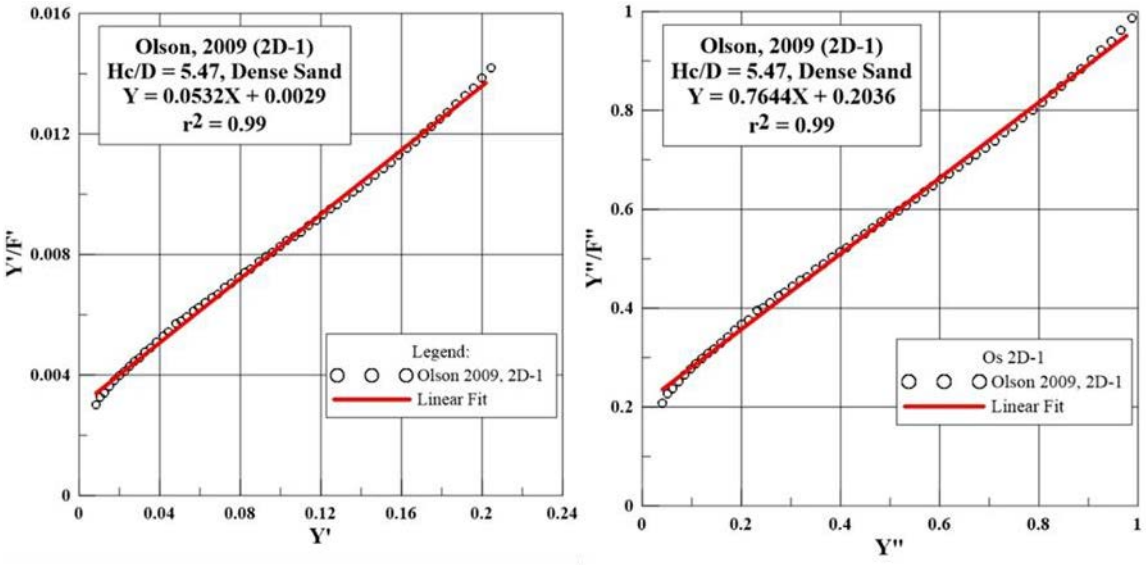

Figure B-8: Olson (2009), Test 2D-1, plotted on a single- (left) and double- (right) normalized transformed axis.

As described by the linear line in Figure A-10, single-normalized (left image), Y = 0.0407X + 0.0053, where A' is 0.0053 and B' is 0.0407. For the linear line provided by double-normalization (right image), Y = 0.7385X + 0.2594, A" parameter is 0.2594 and B" is 0.7385.

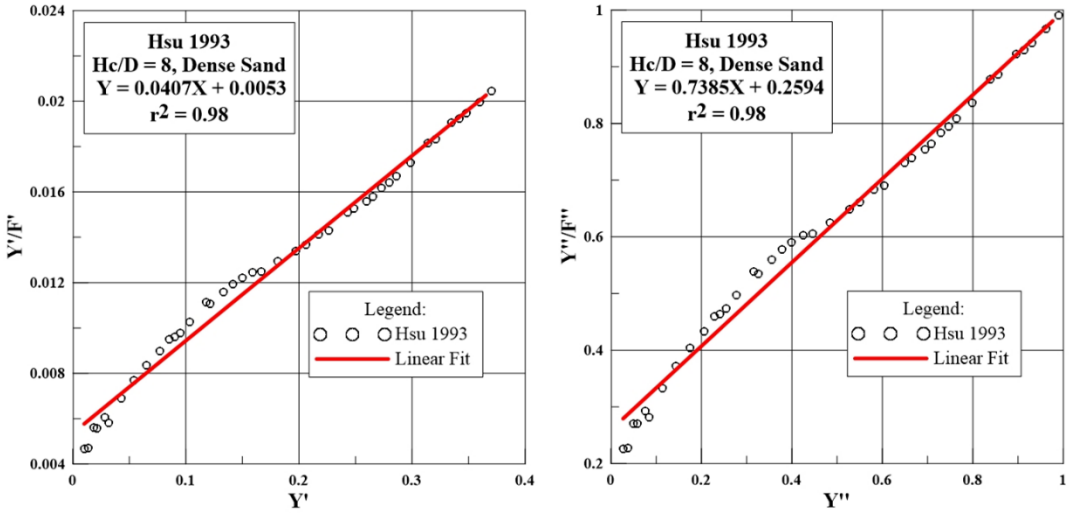

Figure B- 9: Hsu (1993), Hc/D = 8, plotted on a single- (left) and double- (right) normalized transformed axis.

As described by the linear line in Figure A-10, single-normalized (left image), Y = 0.0490X + 0.0034, where A' is 0.0034 and B' is 0.0490. For the linear line provided by double-normalization (right image), Y = 0.8060X + 0.1902, A" parameter is 0.1902 and B" is 0.8060.

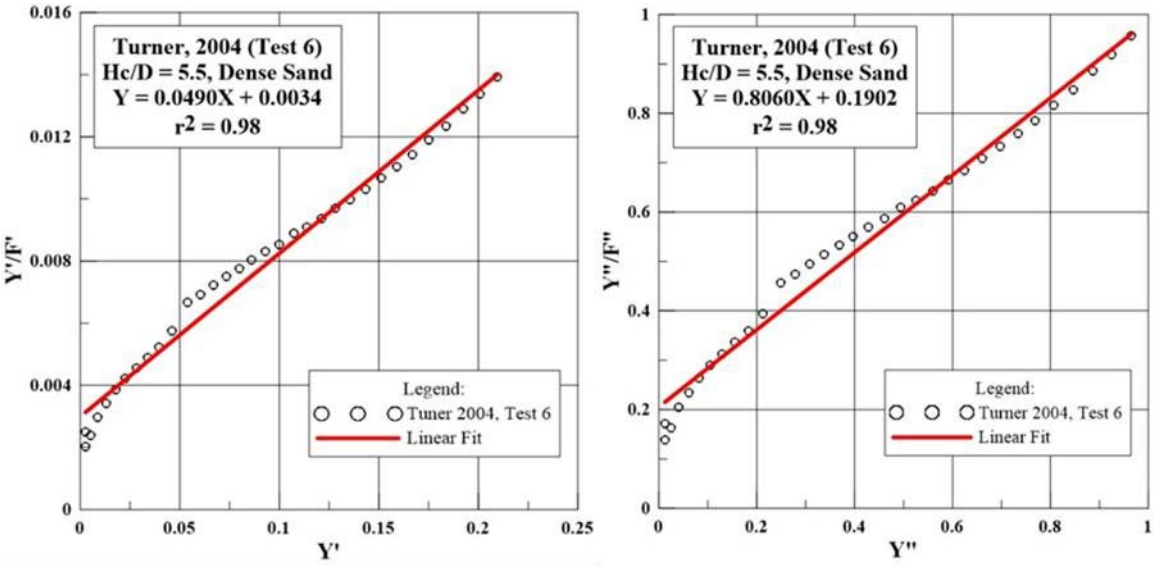

Figure B-10: Turner (2004), Test 6, plotted on a single- (left) and double- (right) normalized transformed axis.

As described by the linear line in Figure A-11, single-normalized (left image), Y = 0.0297X + 0.0032, where A' is 0.0030 and B' is 0.0315. For the linear line provided by double-normalization (right image), Y = 0.6141X + 0.3550, A" parameter is 0.3550 and B" is 0.6141.

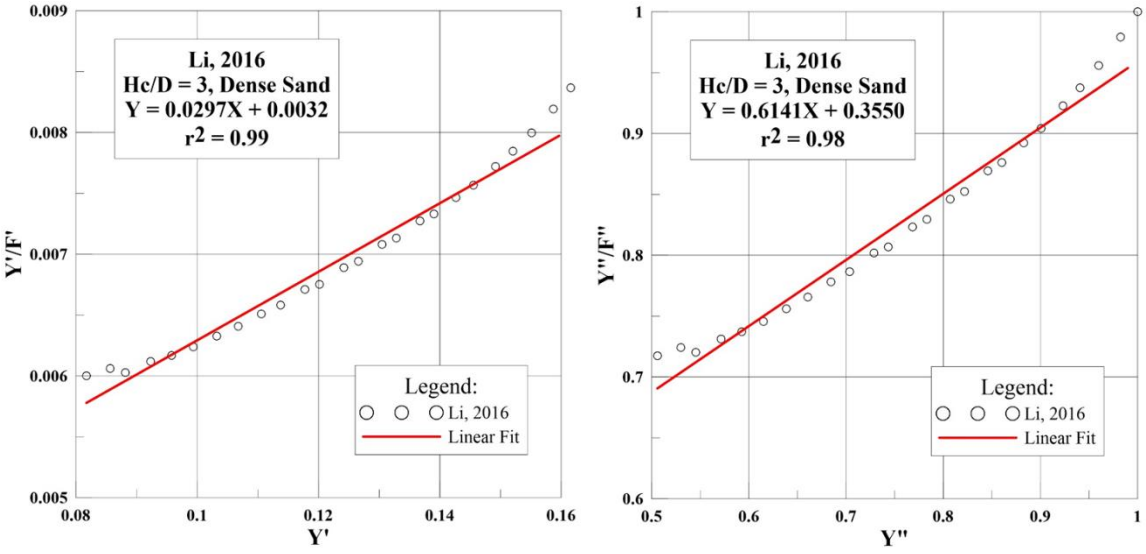

Figure B- 11: Li (2016), Hc/D = 3, plotted on a single- (left) and double- (right) normalized transformed axis

As described by the linear line in Figure A-11, single-normalized (left image), Y = 0.044X + 0.0025, where A' is 0.0025 and B' is 0.0447. For the linear line provided by double-normalization (right image), Y = 0.6660X + 0.2512, A" parameter is 0.2512 and B" is 0.6660.

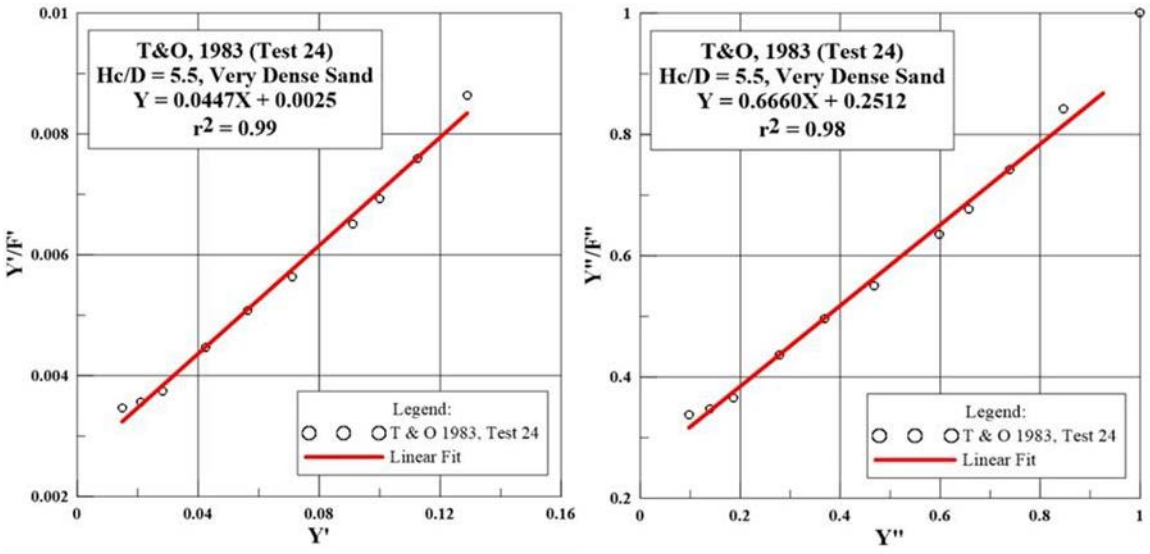

Figure B- 12: Trautmann and O'Rourke (1983), Test 24, plotted on a single- (left) and double- (right) normalized transformed axis.